

1
2
3
4
5
6
7
8
9
10
11
12
13
14
15
16
17
18
19
20
21
22
23
24
25
26
27
28
29
30
31
32
33
34
35
36
37
38
39
40
41
42
43
44
45
46
47
48
49
50
51
52
53
54
55
56
57
58
59
60

1 **Intracellular uptake of EGCG-loaded deformable controlled release liposomes for skin**
2 **cancer**
3
4

For Peer Review Only

1
2
3 5 **ABSTRACT**
4
5

6 Caucasian population groups have a higher propensity to develop skin cancer, and associated
7 clinical interventions often present substantial financial burden on healthcare services.
8
9 Conventional treatments are often not suitable for all patient groups as a result of poor
10 efficacy and toxicity profiles. The primary objective of this study was to develop a
11 deformable liposomal formulation, the properties of which being dictated by the surfactant
12 Tween 20, for the dermal cellular delivery of epigallocatechin gallatein (EGCG), a compound
13 possessing antineoplastic properties. Results demonstrated a significant decrease in liposome
14 deformability index (73.66 ± 8.14 to 37.06 ± 7.41) as Tween 20 loading increased from 0 to
15 10 % w/w, indicating an increase in elasticity. EGCG release over 24-hours demonstrated
16 Tween 20 directly incorporation increased release from $13.7 \% \pm 1.1 \%$ to $94.4 \% \pm 4.9 \%$
17 (for 0 and 10 % w/w Tween 20 respectively). Finally, we demonstrated DilC-loaded
18 deformable liposomes were localised intracellularly within human dermal fibroblast and
19 keratinocyte cells within 2-hours. Thus it was evident deformable liposomes are useful in
20 enhancing drug penetration into dermal cells and would be useful in developing a controlled-
21 release formulation.
22
23
24
25
26
27
28
29
30
31
32
33
34
35
36
37
38

39 21 **KEYWORDS:** Skin cancer; deformable liposomes; dermal release; controlled release;
40
41 22 elastic liposomes
42
43
44
45
46
47
48
49
50
51
52
53
54
55
56
57
58
59
60

1. Introduction

Skin cancer is emerging as an increasing public health problem particularly in developed countries [1]. Currently, 2-3 million non-melanoma skin cancers and 132,000 melanoma skin cancers occur globally each year [2]. The large number of cases diagnosed present as a substantial burden to healthcare services [3, 4, 2]. Despite the fact that the majority of skin cancers are treatable, malignant forms of the cancer results in over 9,000 deaths annually worldwide [5]. Current treatment approaches are limited to local surgery to remove the tumour in addition to topical treatments with cream formulations. However, surgical removal may not be suitable for all patients whilst topical therapies are often linked with poor patient compliance stemming from high dose frequency requirements and unpleasant side effects [6]. In addition, topical treatments may cause skin irritation, weeping, cracking and blistering causing discomfort and pain [7-9].

Strategies for cancer management are focused on chemoprevention and chemoprotection. Existing anticancer agents often demonstrate poor safety profiles in addition to unpleasant side effect profiles, and there is an urgent need for novel agents which are both efficacious and possess a limited toxicity profile to non-malignant dermal tissue [10-12]. One group of compounds that have gained interest recently as novel candidates for this purpose are flavonoids, naturally occurring chemicals abundantly expressed in food and drink, and in particular the green tea catechin, epigallocatechin gallatein (EGCG) which is increasingly being exploited for its chemoprevention properties [13-15]. EGCG has been found to affect specific biological processes that could be exploited as targets for the prevention and treatment of cancer [16], and has been demonstrated to possess properties associated with the induction of apoptosis [17], promotion of cell growth arrest by altering the expression of cell cycle regulatory proteins [17], activation of killer caspases and the

1
2
3 52 suppression of oncogenic transcription factors [18, 19, 15] and pluripotency maintaining
4
5 53 factors [20]. However, the application of naturally occurring compounds as
6
7 54 chemopreventative and chemoprotective strategies for skin cancer management has so far
8
9 55 been received with limited success and this may be largely due to inefficient delivery systems
10
11 56 and limited oral bioavailability of promising agents [21-23]. Consequently, to achieve
12
13 57 maximum clinical efficacy, novel approaches are required to enhance compound
14
15 58 bioavailability, of which dermal delivery is particularly promising.

16
17
18 59 The principle function of mammalian skin is to offer protection from environmental
19
20 60 chemicals and xenobiotics [24]. The penetration of drugs across the skin is significantly
21
22 61 inhibited by the skin's inherent barrier properties [25] thus there is a need to develop carrier
23
24 62 systems to enhance penetrability. To fulfil this goal, when applied topically nanoparticle
25
26 63 mediated delivery systems (e.g. microemulsions, liposomes, ethosomes, deformable
27
28 64 liposomes and solid lipid nanoparticles), would benefit the direct dermal delivery of
29
30 65 compounds across the stratum corneum [26-28]. Additionally, such nano-scale structures are
31
32 66 capable of improving drug loading, enhancing systemic bioavailability, imparting a sustained
33
34 67 release profile and allowing targeted drug delivery [29, 30]. Furthermore, the topical
35
36 68 application of such carriers reduces the incidence of undesirable side effects arising from
37
38 69 systemic administration and enhances systemic absorption of drugs after topical application
39
40 70 with permeation enhancers which irreversibly disrupt the stratum corneum [29, 30].
41
42 71 Controversy however surrounds the use of conventional liposomes due to their large size
43
44 72 preventing skin penetration [31, 28, 32, 33], Gregor Cevc [34] demonstrated that
45
46 73 modification of the chemical composition of the lipid bilayer so as to decrease its Young's
47
48 74 modulus resulted in the formation of deformable liposomes. These are able to gain access to
49
50 75 the viable epidermis by overcoming the physical constraints imposed by the stratum corneum
51
52 76 by diminishing the membrane elastic energy required for the liposome to deform and fit
53
54
55
56
57
58
59
60

1
2
3 77 through an aperture size smaller than their original diameter following which reforming to
4
5 78 their original shape [35, 36, 31]. By being able to change shape and volume at minimal
6
7 79 energetic cost, these structures may penetrate across hydrophilic pathways of intact skin [37,
8
9 80 36]. Deformable liposomes often include additional components designed to make the
10
11 81 membrane more liable to deformation and these are termed edge-activators, typically
12
13 82 including surfactants such as Tweens, bile salts and Myrj [38]. The inclusion of this extra
14
15 83 component destabilises the vesicle bilayers by reducing the amount of energy required to
16
17 84 expand the interface allowing the liposome to become more elastic thus increasing the flux
18
19 85 across the skin [38-40].
20
21
22

23 86 The primary aim of this study was to develop and characterise a deformable
24
25 87 controlled release liposome formulation for targeting toward intracellular uptake into dermal
26
27 88 cells. The objectives of the study were therefore to: (i) assess the impact of the edge-activator
28
29 89 Tween 20 on liposomal formulation size; (ii) characterise resultant liposomes vesicle size,
30
31 90 surface charge and encapsulation efficiency; (iii) quantify deformability of resultant
32
33 91 liposomes using a deformability index (DI); (iv) assess release of EGCG; (v) assess the
34
35 92 deformable liposome stability. ; (vi) assess cellular toxicity of EGCG and (vii) assess
36
37 93 intracellular uptake in human dermal fibroblast and keratinocyte cells.
38
39
40
41
42
43
44

45 95 **2. Materials and methods**

46 47 96 **2.1 Materials**

48
49
50
51 97 Phosphatidylcholine (PC) was obtained from Avanti Polar Lipids. Cholesterol, Tween
52
53 98 20 and EGCG were obtained from Sigma-Aldrich. All other reagents including methanol and
54
55 99 chloroform were obtained from Fisher Scientific. Ultrapure water was obtained from a Milli-

1
2
3 100 Q purification system (Millipore, Billerica, MA, US). Human dermal fibroblasts (HDFa)
4
5 101 isolated from adult skin and all cell culture reagents (Medium 106 and low serum growth
6
7 102 supplement (LSGS) kit containing supplemented medium containing foetal bovine serum, 2
8
9 103 % v/v, hydrocortisone 1 µg/mL, human epidermal growth factor, 10 ng/mL, basic fibroblast
10
11 104 growth factor, 3 ng/mL, heparin, 10 µg/mL; DMEM media supplemented with 1 % L-
12
13 105 glutamine, 10 % FBS, 1 % Penicillin Streptomycin and 0.25% amphotericin) were obtained
14
15 106 from Life technologies (Carlsbad, California, US). Immortalized human keratinocytes
16
17 107 (HaCat) cells were a kind gift from Dr Andrew Sanders (Cardiff China Medical Research
18
19 108 Collaborative, Cardiff University, Henry Wellcome Building, Heath Park, Cardiff, CF14
20
21 109 4XN).

25 110 **2.2 Methods**

28 111 *2.2.1 Preparation of deformable liposomes with or without an edge activator*

31 112 Liposomes were prepared by adapting the film hydration method established by
32
33 113 Bangham *et al.*, (1965) [41]. PC and cholesterol (16:8 µM) were dispersed in an organic
34
35 114 solvent mixture consisting of chloroform and methanol in a 9:1 ratio in a round bottomed
36
37 115 flask [40, 38, 26, 42, 41]. Subsequently, the organic solvent was removed by rotary
38
39 116 evaporation for 5 minutes at 35 °C, followed by purging with nitrogen gas. The resultant dry
40
41 117 film residue was hydrated by the addition of 4 mL water containing edge activator (up to 10%
42
43 118 w/w of the formulation) and 1 mg of EGCG at a temperature above the transition temperature
44
45 119 of the phospholipid (between -7 to -15°C) [43] and vortexed for 5 minutes to form
46
47 120 multilamellar vesicles (MLV). The resulting particles were extruded 21 times through 100-
48
49 121 nm diameter polycarbonate membranes, using an Avanti Mini Extruder to produce
50
51 122 unilamellar vesicles. The formed liposomes were equilibrated for 30 min above their
52
53 123 transition temperatures (-15°C) before being subjected to further characterisation [44, 45, 43].
54
55
56
57
58
59
60

1
2
3 1244
5
6 125 *2.2.2 Deformable liposome characterisation*
7

8
9 126 The mean particle size and the polydispersity index (measurement of the level of
10
11 127 homogeneity of particle sizes) of liposomes were measured by dynamic light scattering
12
13 128 (DLS) using a Zetaplus (Brookhaven Instruments) following dilution with distilled water (1:4
14
15 129 ratio) to ensure intensity adjustment. A polydispersity value of < 0.2 indicates a homogenous
16
17 130 vesicle population, while polydispersity of > 0.3 indicates heterogeneity [46]. The particle
18
19 131 charge was quantified as zeta potential (ζ). Zeta potential was determined by photon
20
21 132 correlation spectroscopy using a Zetaplus (Brookhaven Instruments). The samples were
22
23 133 diluted three-fold and assessed in triplicate.

24
25
26
27 134 *2.2.3 HPLC-UV detection of EGCG*
28

29
30 135 Detection of EGCG was assessed using reverse phase HPLC methodology. A Waters
31
32 136 Alliance separation module HPLC with UV detection was utilised at an operating wavelength
33
34 137 of 275 nm [47] with a Waters X select column (5 μ m C18 4.6 x 150 mm), with a 10 μ L
35
36 138 injection volume. The mobile phase comprised of a 70:30 ratio of 0.1% TFA in water to
37
38 139 methanol at a flow rate of 1 mL/min. Stock solutions and standard solutions of EGCG were
39
40 140 prepared with both water and ethanol ranging from 0.5-500 μ g/mL. A final A calibration
41
42 141 curve with an R^2 of 0.997 and linear equation of $y = 1 \times 10^7 \cdot x$ was obtained.
43
44
45

46 142 *2.2.4 Entrapment efficiency of EGCG*
47

48
49 143 The entrapment efficiency of EGCG loaded deformable liposomes was determined by
50
51 144 centrifuging samples and quantifying the EGCG in the supernatant. Samples were centrifuged
52
53 145 at 18,000 rpm for 30 min at 4°C in an Optima[™] MAX-XP ultracentrifuge to separate the
54
55
56
57

1
2
3 146 incorporated drug from the free drug. The supernatant was then analysed using HPLC to
4
5 147 determine the encapsulation efficiency of EGCG in liposomal formulations (Equation 1):
6
7

8 148
$$E = \frac{D_t - D_s}{D_t} \times 100\% \quad (1)$$

9

10
11
12 149 where E is the encapsulation efficiency (%), D_t is the total drug content (mg) and D_s is drug
13
14 150 content in supernatant (mg).
15

16 17 151 *2.2.5 Assessment of liposomal deformability*

18
19
20 152 To assess the deformability of formulated liposomes, a liposome suspension (6 mL)
21
22 153 consisting of a 16:8 micromolar ratio of PC to cholesterol formulated with up to 10% w/w of
23
24 154 Tween 20 solution (diluted 3 fold), was passed through a polycarbonate filter of 50 nm pore
25
26 155 size using a syringe driver (Cole Parmer, UK) set at 0.6 mL/min for 10 min. The mean
27
28 156 particle size and the polydispersity index of liposomes were subsequently quantified by DLS,
29
30 157 before and after filtration, to assess the ability of formulated liposomes to regain their size
31
32 158 after having been forced through a pore size smaller than their original diameter. The
33
34 159 deformability was quantified through the calculation of a deformability index (equation 2)
35
36 160 [32]:
37
38
39

40
41 161
$$D = 100 - \frac{L_e}{L} \times 100 \quad (2)$$

42
43

44 162 where D is deformability, L_e is size of extruded liposomes (nm), L is size of liposomes (nm)
45
46 163 prior to extrusion.
47

48 49 164 *2.2.6 Differential scanning calorimetry of EGCG and EGCG lipid blends*

50
51
52 165 To assess thermal characteristics of materials including melting temperatures, phase
53
54 166 transitions and heat capacity changes of liposomes, EGCG and ratios of lipid, surfactant and
55
56
57

1
2
3 167 drug mixtures corresponding to that of the liposome formulation, were analysed in the solid
4
5 168 state using a TA Instruments Q200 Thermal Analysis Differential scanning calorimetry
6
7 169 (DSC). 3 mg of EGCG was weighed into T-Zero aluminium pans and then hermetically
8
9 170 sealed. All experimental runs commenced at an initial temperature of 0°C, purged under
10
11 171 nitrogen gas, with a scan rate of 10°C/min to 300°C.

12 13 14 172 *2.2.7 In-vitro EGCG release studies*

15
16
17 173 To assess the impact of inclusion of Tween 20 on EGCG from liposomal formulations, a
18
19 174 side—by-side diffusion cell (PermeGear diffusion cell, Hellertown, USA) was maintained at
20
21 175 35 °C. Release was assessed over a 24 hour period from an EGCG aqueous solution (0.1
22
23 176 mg/mL) and EGCG-loaded liposomes (final loading for liposomes formulated with 0, 2, 6
24
25 177 and 10 % w/w Tween 20 was 0.80, 0.55, 0.17 and 0.04 mg/mL respectively). 10 mL of each
26
27 178 formulation was placed into the donor side of the diffusion cell and release across a 50 nm
28
29 179 membrane (Whatman®) into the receiver side containing 100 mL of dermal dissolution
30
31 180 media with a stirrer was measured. The release media was sampled with volume replacement
32
33 181 (0.5 mL) over 24 hours and analysed using HPLC-UV quantification.

34 35 36 37 38 182 *2.2.8 In-vitro drug release kinetics*

39
40
41 183 Several kinetic drug release mathematical models were used to assess drug release from the
42
43 184 formulations. The best-fit to the mathematical models described below confirmed the
44
45 185 appropriate release kinetics:

46
47
48 186 *Zero order model:* $\frac{M_t}{M_\infty} = k_0 \cdot t$ (3)
49
50

51
52 187 where M_t/M_∞ is the drug fraction released at time t and k_0 is the zero-order release constant.

53
54
55 188 *First order model:* $\frac{M_t}{M_\infty} = 1 - e^{-k_1 t}$ (4)
56
57

1
2
3 189 where M_t/M_∞ is the drug fraction released at time t and k_1 is the first-order release constant.

4
5
6 190 Higuchi model: $\frac{M_t}{M_\infty} = k_H \cdot t^{\frac{1}{2}}$ (5)
7

8
9
10 191 where M_t/M_∞ is the drug fraction released at time t and k_H is the Higuchi constant.

11
12
13 192 Korsmeyer-Peppas Model: $\frac{C_t}{C} = Kt^n$ (6)
14

15
16 193 where C_t/C is fraction of drug released at time t , k is the release rate constant. The value of n
17
18 194 is valuable in understanding drug release mechanisms. When $n \leq 0.45$ drug release is
19
20 195 diffusion controlled and can be referred to as 'Fickian' diffusion and when $n > 0.89$ the
21
22 196 diffusion is indicative of erosion controlled drug release or class-II kinetics. For situations
23
24 197 where $0.45 < n \leq 0.89$ the diffusion is a complex mixture of both processes and often termed
25
26 198 anomalous transport. In all cases this is based on the assumption of release from a cylinder
27
28 199 and applied to cumulative release rates $< 60\%$ [48]

29
30
31
32 200 Mathematical models to assess release kinetics were fit using Microsoft Excel[®]. Zero order,
33
34 201 first order, Higuchi and Korsmeyer-Peppas release profiles were applied to release from drug
35
36 202 solution and drug loaded liposome solution following which regression analysis techniques
37
38 203 were employed to determine the probable drug-release. The release kinetic model displaying
39
40 204 the highest r^2 metric (≥ 0.95) was determined to be the mechanism, by which release occurred.

41 42 43 44 205 2.2.9 Liposome stability

45
46
47 206 The stability of liposomes was determined, as prepared in water, through the assessment of
48
49 207 particle size over a 28-day period, stored in a stability cabinet maintained at 25 ± 2 °C
50
51 208 (Firlabo, France) at a humidity of $60\% \pm 5\%$. Mean particle sizes were determined on days
52
53 209 1, 2, 7, 14, 21 and 28 by DLS. Furthermore, the encapsulation efficiency of drug loaded
54
55 210 liposomes was assessed over 4 weeks as detailed in section 2.2.4.

1
2
3 2114
5
6 2127
8
9 213 *2.2.10 Development of an in-vitro cellular dermal model*

10
11
12 214 To develop an *in-vitro* system to assess cellular toxicity and cellular uptake of
13
14 215 deformable liposomes into representative human dermal tissue, two dermal cell line were
15
16 216 examined. Human dermal fibroblasts (HDFa) were cultured in Medium 106 supplemented
17
18 217 with low serum growth supplement. Human epidermal keratinocytes (HaCaT) cells were
19
20 218 revived and sustained in high glucose supplemented DMEM media. Media was replaced
21
22 219 every 3 days. At 70-80% confluency, media was discarded and cells detached using
23
24 220 Trypsin/EDTA incubated for 5 min, prior to trypsin neutralisation with 3 mL growth media
25
26 221 and subsequent centrifugation at 1200 rpm for 10 min and resuspension in fresh media prior
27
28 222 to being utilized for subsequent studies

29
30
31
32 223 *2.2.11 Cellular toxicity of liposomal formulations towards HDFa and HaCat cells*

33
34
35 224 To determine the cytotoxicity profile of EGCG towards HDFa and HaCat cells, a
36
37 225 (2,3-Bis-(2-Methoxy-4-Nitro-5-Sulphophenyl)-2H-Tetrazolium-5-Carboxanilide (XTT) assay
38
39 226 [49] was performed to measure cell viability after exposure to increasing concentrations of
40
41 227 EGCG for 24 hours. Cells were seeded at a density of 50×10^3 cells per well into a 96-well
42
43 228 plate and grown for 3 days. Thereafter, media was removed and cells were exposed to 100 μ L
44
45 229 of 0.1-100 μ M EGCG and incubated for 24 hours at 37°C. Subsequently, 25 μ L of a 12.5:1
46
47 230 (XTT: menadione) was added each well and incubated for 3 hours at 37°C prior to the
48
49 231 absorbance being read at 450 nm. Assessment of EGCG toxicity to these cells was conducted
50
51 232 through analysis of changes in XTT absorbance with increasing drug concentration.

52
53
54
55 233 *2.2.12 Intracellular uptake of deformable liposomes into HDFa and HaCat cells*

1
2
3 234 Liposomes, both deformable and non-deformable, were formulated with the addition of 0.25
4
5 235 mL of a 0.1 mg/mL DilC during the lipid mixing stage. Unentrapped DilC was removed by
6
7 236 centrifuging liposomes at 18,000 g for 30 min. Coverslips were coated for 30 min with poly-
8
9 237 l-lysine (0.01 % w/v) prior to the addition of cells at a density of 50×10^3 cells per coverslip.
10
11 238 After 24 hours, DilC loaded liposomes were diluted with 1 part of supplemented media (as
12
13 239 clarified in materials) and were then added to the coverslips and incubated for 2 hours at
14
15 240 37°C.

16
17
18 241 Thereafter, coverslips were washed and fixed with 4 % w/v paraformaldehyde for 5 minutes
19
20 242 at room temperature. Subsequently, coverslips were mounted onto glass slides with the
21
22 243 addition of a DAPI-containing mounting media. Cover slips were subsequently analysed in
23
24 244 an upright confocal microscope (Leica SP5 TCS II MP) and visualised with a 40× oil
25
26 245 immersion objective. Images were acquired using a helium-neon laser at 633 nm to visualise
27
28 246 DilC and a helium–neon laser to visualise DAPI at 461 nm.

29 30 31 32 247 *2.2.13 Statistical analysis*

33
34
35 248 Unless otherwise stated, all results are presented as mean \pm standard deviation (SD).
36
37 249 Replicates of at least 3 were used for all studies. For multiwell plate assays replicates of 6
38
39 250 were used for each experimental condition with the study replicated 3 times. A one-way
40
41 251 ANOVA was used to determine any statistically significant difference between means tested.
42
43 252 A post-hoc Tukey's multiple comparisons test was then applied to assess differences between
44
45 253 groups. All the calculations were carried out using Graphpad 6 (GraphPad Inc., La Jolla,
46
47 254 CA).

48 49 50 51 52 255 **3. Results and discussion**

1
2
3 256 Emerging treatments for cancer management involve chemoprevention and chemoprotection.
4
5 257 Current anticancer agents tend to demonstrate a poor safety profile in addition to possess a
6
7 258 wide range of unpleasant side effects [10-12]. However, phytochemical flavonoids, such as
8
9 259 EGCG, are increasingly being investigated for their chemoprevention properties [13-15].

10
11
12 260 EGCG is a flavonoid found in green tea that possesses cytotoxic effects in cancerous skin
13
14 261 cells and thus may be a potentially viable candidate as a pharmacological anti-cancer agent
15
16 262 [16], given that it has been observed to induce apoptosis in cancer cells without affecting
17
18 263 normal cells [50, 17], in addition to the modulating expression of a number of genes involved
19
20 264 in cell proliferation, cell-cell contact and cell-matrix interactions [51].

21
22
23
24 265 However, the penetration of drugs across the skin is significantly hindered by the skin's
25
26 266 inherent barrier properties [25]. The use of deformable liposomes to aid dermal cellular
27
28 267 penetrability and uptake may be advantageous in the targeting of neoplastic agents to deeper
29
30 268 skin cellular layers when compared to conventional liposomes which may not be able to
31
32 269 penetrate through the narrow pore of the stratum corneum [39].

33
34
35
36 270 This focus of this study was to develop EGCG loaded slow release deformable liposomes.
37
38 271 EGCG liposomes were formulated with PC and cholesterol with the inclusion of Tween 20 as
39
40 272 a edge-activator with incorporation of up to 10 % w/w. Liposomal characteristics including
41
42 273 liposome size, charge, encapsulation efficiency, DI, release profile, stability, ceulluar toxicity
43
44 274 and uptake were was assessed.

45 46 47 275 ***3.1 Liposome characterisation***

48
49
50
51 276 The impact of the inclusion of Tween 20 within the liposomal formulation on
52
53 277 liposome characteristics were observed. As the surfactant loading in the bilayer of 'empty'
54
55 278 liposomes increased, liposome diameter decreased from 206.45 ± 24.33 nm for liposomes

1
2
3 279 formulated with no surfactant to 101.61 ± 11.27 nm for liposomes formulated with 10 % w/w
4
5 280 Tween 20 (Figure 1A). As the surfactant loading in the bilayer of EGCG loaded liposomes
6
7 281 increased, liposome diameter decreased, from 258.43 ± 16.69 nm for liposomes formulated
8
9 282 with no surfactant compared with 104.95 ± 12.56 nm for liposomes formulated with 10 %
10
11 283 w/w Tween 20 (Figure 1B). The decrease in size was statistically significant for ‘empty’ and
12
13 284 EGCG loaded liposomes formulated with no surfactant compared with liposomes loaded with
14
15 285 2, 6 and 10 % w/w Tween 20.

16
17
18
19 286 [Figure 1 near here]

20
21
22 287 The inclusion of surfactants into liposome formulations have previously been demonstrated
23
24 288 to decrease liposome size when compared to liposomes formulated in the absence of
25
26 289 surfactant [26, 32]. This may be as a result of a destabilising effect imparted by the surfactant
27
28 290 on the bilayer [52], which results in a greater interaction of the phospholipid bilayer with the
29
30 291 aqueous phase. A consequence of this would then be the overall formation of liposomes with
31
32 292 a smaller diameter giving a greater surface area in contact with the aqueous phase. The
33
34 293 inclusion of surfactant has been previously reported to decrease liposome size in comparison
35
36 294 to conventional liposomes. A study formulating liposomes with Phospholipon® 90 G and
37
38 295 both Tween 80 and Span 80 reported a size reduction from 207 nm to 139 nm following
39
40 296 inclusion of the surfactants [32].

41
42
43
44 297 A liposome preparation which is homogenous in size is important as final liposome
45
46 298 size will partly determine the level of tissue distribution *in-vivo* in addition to influencing
47
48 299 drug release kinetics. A polydispersity of up to 0.3 is considered homogenous [53, 32, 54]. As
49
50 300 the loading of surfactant increased, the polydispersity of the liposomal formulation decreased,
51
52 301 non-significantly from 0.33 to 0.27 and significantly ($P < 0.$) 0.32 to 0.22 for ‘empty’

1
2
3 302 liposomes (Figure 1a) and those loaded with EGCG respectively (Figure 1b). Therefore, the
4
5 303 inclusion of Tween 20 within the liposome formulation appeared to improve homogeneity.
6
7

8 304 The magnitude of the zeta potential (ζ) indicates the degree of electrostatic repulsion
9
10 305 between adjacent, similarly charged particles in a dispersion. Thus, it is a fundamental
11
12 306 parameter thought to affect stability of liposomal formulations. All formulated liposomes
13
14 307 demonstrated a near neutral charge (Table 1). A neutral liposomal surface charge is important
15
16 308 to avoid skin irritation [55] however, this may subsequently lead to particle flocculation due
17
18 309 to attractive forces between liposomes causing them to cluster [56].
19
20

21
22 310 [Table 1 near here]
23
24

25 311 In liposomes formulated with EGCG, as Tween 20 loading increased, a statistical
26
27 312 significant decrease in EGCG entrapment was observed, ($P \leq 0.0001$), from 80.0 ± 3.0 % no
28
29 313 surfactant to 4.3 ± 3.0 % with a 10 % w/w loading of surfactant (Figure 2). This decrease in
30
31 314 EGCG loading may be related to the difference in the molecular weight of EGCG and Tween
32
33 315 20. Tween 20, with larger molecular weight of 1227.54 g/mol compared to that of EGCG
34
35 316 (386.65 g/mol), may be assumed to be better poised to displace EGCG from the bilayer.
36
37 317 Further, the hydrophobic tail of Tween 20 would have a high affinity to the chains in PC
38
39 318 therefore displacing EGCG from the bilayer [57-59]. Furthermore, Tween 20 is known to
40
41 319 enhance the solubility of drugs and therefore, as not all would be entrapped within the
42
43 320 bilayer, this may allow increased EGCG solubilisation within the liposomal rehydration
44
45 321 media [60]. It is also possible that the coexistence of vesicles and mixed micelles at high
46
47 322 surfactant concentrations [61] may have reduced the compound entrapment in mixed
48
49 323 micelles.
50
51

52
53
54 324 [Figure 2 near here]
55
56
57
58
59
60

1
2
3 325 The degree of deformability of each formulation was determined by extrusion through
4
5 326 a polycarbonate filter with a pore size of 50 nm. The mean particle size and the polydispersity
6
7 327 index of liposomes was quantified before and after filtration to assess liposome ability to
8
9 328 regain size after having being forced through a pore size smaller than their original diameter.
10
11 329 The DI is defined as the degree the liposomes deformed; the greater the degree of
12
13 330 deformation the less elastic the liposomes are as they were unable to regain their previous
14
15 331 larger size. The DI following extrusion decreased with statistical significance ($P \leq 0.0001$) as
16
17 332 surfactant loading increased in 'empty' liposomes, from 70.8 ± 6.5 to 25.6 ± 2.9 % for
18
19 333 liposomes formulated with no surfactant compared with 25.6 ± 2.93 for liposomes formulated
20
21 334 with 10 % w/w Tween 20 respectively. EGCG liposomes formulated with Tween 20
22
23 335 demonstrated a statistically significant decrease ($P \leq 0.0001$) in DI from 73.66 ± 8.14 for
24
25 336 liposomes formulated with no surfactant compared with 37.06 ± 7.41 for liposomes
26
27 337 formulated with 10 % w/w Tween 20 (Figure 3). These observations imply the liposomes
28
29 338 were displaying elastic properties as they could deform in order to pass through an opening
30
31 339 smaller than its own diameter whilst, to a certain degree regaining its size. Additionally, the
32
33 340 presence of EGCG in the liposome formulation did not appear to affect the DI compared with
34
35 341 liposomes formulated without. A study formulating liposomes with Phospholipon® 90 G and
36
37 342 both Tween 80 and Span 80 saw a size reduction observed surfactant to decrease the DI from
38
39 343 51.4 ± 3.6 to 17.3 ± 5.2 [32].
40
41
42
43
44

45 344 [Figure 3 near here]
46
47

48 345 Liposomes formulated with surfactant can deform as the surfactant has a propensity
49
50 346 for highly curved structures (e.g. micelles and liposomes), thus diminishing the energy
51
52 347 required for particle deformation. The surfactant is able to diminish the energy required for
53
54 348 particle deformation and accommodate particle shape changes of the liposomes under stress
55
56
57

1
2
3 349 [62]. These surfactants may have interacted with the PC with strong affinity but in reversible
4
5 350 mode. The reversible binding mode might have provided the deformability upon physical
6
7 351 stress [38].
8
9

10 352 For liposomes to deform, a source of energy is required [63-65]. In our
11
12 353 systems, 'energy' was supplied to this system in the form of pressure as a result of the action
13
14 354 of the syringe driver. The larger the concentration of surfactant included within the
15
16 355 formulation, the greater the energy the liposome as a whole is able to retain [65]. It is
17
18 356 postulated that this energy is used to reorientate the lipid bilayer structure, and since all
19
20 357 systems tend toward the lowest state of free energy, the energy stored in this structure will be
21
22 358 expelled once the liposome has passed through the pore and there is no longer any pressure
23
24 359 forcing the bilayer to remain in an 'unnatural state' [35, 36, 66]. This energy can then be
25
26 360 expended into reforming the liposome. Some energy will be lost during passage as heat or
27
28 361 non-plastic deformation, therefore it was not possible to attain a DI of 0 %.

31
32 362 The energy used to alter the bilayer of a liposome containing no surfactant does not benefit
33
34 363 from the extra 'storage space' of a surfactant, thus energy may be expended to rupture the
35
36 364 membrane causing liposome size to decrease [65]. Despite the potential for excess energy in
37
38 365 liposomes formulated with Tween 20, liposomes were not able to fully regain their pre-
39
40 366 extrusion size. Some energy will always be lost in the friction of the particles moving through
41
42 367 the pores as heat [67]. An increase in surfactant loading may bring the liposomes closer to
43
44 368 100% reformation [65]. Further, liposomes unable to fit through the pores or lipid aggregates
45
46 369 from ruptured liposomes may cause blockages. This may lead to an increase in pressure in the
47
48 370 vessel causing more turbulence leading to the rupture and non-uniform reformation of
49
50 371 liposomes. Additionally, *in-vivo*, liposomes would be expected to move across the skin
51
52 372 following an osmotic transepidermal gradient as has been reported in many similar studies
53
54
55
56
57
58
59
60

1
2
3 373 concerning the dermal and transdermal delivery of drug [64, 39, 65, 32]. Such lipid carriers
4
5 374 are miscible with the epidermal lipids present within the barrier of the stratum corneum thus
6
7 375 would be able to penetrate into deeper layers of the skin [68-70]. Furthermore, the skin is
8
9 376 warmer than room temp (35 °C compared to 20 °C). Temperature governs the energy term of
10
11 377 enthalpy therefore the liposomes would have more energy to be even more flexible and cross
12
13 378 the stratum corneum. M.

16 379 ***3.2 Differential scanning calorimetry investigations of EGCG and EGCG lipid blends***

19
20 380 Differential scanning calorimetry (DSC) has been widely used in understanding the
21
22 381 thermal characteristics of materials where an insight into a range of thermal properties
23
24 382 including melting temperatures, phase transitions and heat capacity changes can be obtained.
25
26 383 It has been observed that drugs with melting point of < 200 °C are better poised to cross the
27
28 384 SC [71, 24], therefore observing the effect of formulation parameters on the melting point
29
30 385 would aid formulation development. The glass transition temperature (T_c) of EGCG was
31
32 386 identified at 220 °C (peak c) and the melting point (T_m) of EGCG was at 245 °C (peak d)
33
34 387 (Figure 4) and concurred with those reported by Cho et al (2008) where the T_m of GCG (an
35
36 388 epimer of EGCG) was at 223 °C, the T_c of EGCG was at 235 °C and the T_m of EGCG was at
37
38 389 246 °C. Cho et al also observed a peak at 97 °C and determined it to be the conversion
39
40 390 temperature of EGCG into GCG. Therefore, the first two troughs (peak a and b) observed in
41
42 391 the scan may be representative of the epimer GCG [72].

43
44
45
46
47 392 [Figure 4 near here]

48
49
50 393 The DSC of the lipid (PC and cholesterol) and Tween 20 blend observed the T_m of
51
52 394 this mixture to be 172 °C (Figure 5A). Upon addition of EGCG to this mixture, the melting
53
54 395 point shifted to 191 °C (Figure 5B), illustrating that the surfactant loaded liposomes could
55
56 396 decrease the T_m of EGCG thus potentially improving partitioning across the skin [73].

1
2
3 397 [Figure 5 near here]
4
5

6 398 **3.3 EGCG release studies from liposomal formulations**
7

8
9 399 The release of EGCG from solution and liposomal formulations was studied over a 24-hour
10
11 400 period (Figure 6). Liposomes appeared to retard the release of EGCG in comparison to
12
13 401 release across the membrane from EGCG in solution. Furthermore, with increasing the
14
15 402 loading of Tween 20 within liposomal formulations (0 to 10 % w/w), EGCG release
16
17 403 increased from 13.65 ± 1.12 % at 24 hours for 0 % w/w Tween 20, to 94.37 ± 4.90 % at 24
18
19 404 hours for 10 % w/w Tween 20. The cumulative percentage released after 24 hours was
20
21 405 significant between the solution and liposomes loaded with 0%, 2%, and 6% w/w of Tween
22
23 406 20 ($P \leq 0.0001$). The inclusion of surfactant enables an increase in drug solubility of poorly
24
25 407 soluble compounds thus explaining the increase in drug release at higher loadings of
26
27 408 surfactant. Such properties are already exploited to improve the oral delivery release profiles
28
29 409 of poorly soluble compounds in self-emulsifying drug delivery systems with four drug
30
31 410 products [74, 75], Sandimmune® and Sandimmun Neoral® (cyclosporin A), Norvir®
32
33 411 (ritonavir), and Fortovase® (saquinavir) on the pharmaceutical market [74]. It is worth noting
34
35 412 that as surfactant loading increased, EGCG entrapment decreased thus a lower concentration
36
37 413 gradient would be observed. This did not appear to retard EGCG release.
38
39
40

41
42 414 [Figure 6 near here]
43
44

45
46 415 An increased rate of release was observed from the EGCG solution compared with
47
48 416 liposome formulations over the 24 hours observed (Table 2). Further, as the loading of
49
50 417 surfactant increased, the rate of EGCG release increased (from 0.034 ± 0.013 to $0.993 \pm$
51
52 418 1.013 for liposomes loaded with 0 % and 10 % of Tween 20 respectively based on the
53
54 419 Korsmeyer-Peppas model). Thus, surfactant appears to increase drug release, particularly at
55
56 420 10 % w/w where the rate was 10 fold greater than that at 6% w/w. The surfactant would
57
58
59

1
2
3 421 increase drug solubility thus explaining why an increase in drug release is observed at higher
4
5 422 loadings of surfactant. The inclusion of surfactant destabilizes the vesicle bilayers by
6
7 423 reducing the amount of work required to expand the interface allowing the liposome to
8
9 424 become more flexible [40, 38, 39] and move through the membrane. Additionally, it has been
10
11 425 suggested that the mechanism of the *in-vitro* release seems to be the formation of transient
12
13 426 pores in the lipid bilayer, through which drugs are released to the extra-liposomal medium
14
15 427 (Wang, Wang et al. 2016).

16
17
18
19 428 [Table 2 near here]

20
21
22 429 Based on the values of the determination coefficient (R^2), as well as AIC values
23
24 430 (Akaike Information Criterion), the model that best describes EGCG release from all
25
26 431 liposomal formulations is Korsmeyer-Peppas model (highest R^2 and lowest AIC). The
27
28 432 diffusion release exponent value revealed a range of release mechanisms for each
29
30 433 formulation. Liposomes formulated with 0%, 6 % and 10% w/w Tween 20 had an exponent
31
32 434 value of 0.839 ± 0.072 , 0.836 ± 0.116 and 0.722 ± 0.247 respectively indicating the release is
33
34 435 a complex mixture of the diffusion (flux due to molecular diffusion and the concentration
35
36 436 gradient) and erosion controlled drug release or class-II kinetics (diffusion not based on
37
38 437 concentration gradient) processes and often termed anomalous transport [76]. Liposomes
39
40 438 formulated with 2 % w/w Tween 20 observed an exponent value of 0.913 ± 0.186 indicative
41
42 439 of erosion controlled drug release or class-II kinetics [48].

43 440 **3.4 Stability of EGCG loaded deformable liposomes**

44
45
46
47
48
49
50 441 The impact of long-term storage of EGCG-loaded liposomes formulated with 2 %
51
52 442 w/w Tween 20 was assessed during storage in stability cabinets maintained at 25 ± 2 °C
53
54 443 (Firlabo, France) at a humidity of $60 \% \pm 5$ %. Liposomes formulated with 2% w/w Tween
55
56 444 were selected in this study as it had the highest EGCG entrapment compared with the higher

1
2
3 445 loadings of surfactant thus will be taken forward for cell uptake studies. The impact of this
4
5 446 storage on size (Figure 7) and encapsulation efficiency (Figure 8) was assessed. EGCG
6
7 447 loaded liposomes formulated with and without surfactant maintained a consistent size over
8
9 448 time (Figure 7) with no statistically significant difference in size during the storage period.
10
11 449 Previous reports have highlighted that aggregation is common upon liposomal formulation
12
13 450 storage, and results in vesicle size growth [77] particularly with neutral liposomes [56].
14
15 451 However, the inclusion of Tween 20 into the deformable liposomes may have prevented this
16
17 452 phenomenon and may be a result of surfactant destabilising the lipid bilayer and reducing the
18
19 453 energy required to expand the interface, thus allowing maintenance of smaller structures. It
20
21 454 appears the inclusion of surfactant prevents this phenomenon which correlates with similar
22
23 455 studies [78].

24
25
26
27 456 [Figure 7 and 8 near here]

28
29
30 457 Furthermore, encapsulation efficiency appears to decrease non-significantly from $43.02 \pm$
31
32 458 6.82% to $42.29 \pm 11.63 \%$, $38.76 \pm 9.08 \%$, $30.38 \pm 11.18 \%$ to $30.33 \pm 6.42 \%$, for
33
34 459 liposomes formulated with 2 % w/w Tween 20 (Figure 8). This suggests drug leaching is
35
36 460 independent of surfactant loading. However, Tween 20 is able to increase compound
37
38 461 solubility, therefore, as not all would be entrapped within the bilayer, this may allow EGCG
39
40 462 to solubilise within the liposomal media [60]. Therefore, as the loading of Tween 20
41
42 463 increased, this would increase the amount of free Tween 20 resulting in more EGCG being
43
44 464 able to solubilise in the liposome media.
45
46
47
48

49 465

50
51
52 466 ***3.5 Cellular toxicity of liposomal formulation towards HDFa and HaCat cells***
53
54
55
56
57

1
2
3 467 Whilst topical formulations are applied directly into the skin, various connective layers
4
5 468 making up the skin are important for drug delivery. The skin primarily consists of the
6
7 469 epidermis, dermis and subcutaneous layers and each layer has a unique combination of cells,
8
9 470 connective tissue, components and functions. Skin cancers develop in the upper layers of the
10
11 471 skin spanning the dermal and epidermal layer, and any formulation system should consider
12
13 472 the impact of formulation systems on these tissue layers for the delivery of drugs.
14
15

16 473 In order to assess cellular toxicity of EGCG to these cells, we adopted two *in-vitro* cell
17
18 474 culture systems, namely human keratinocyte and human fibroblast cells. To determine the
19
20 475 cellular viability cytotoxicity of EGCG towards HDFa and HaCat cells, an XTT assay was
21
22 476 performed to measure cell death after exposure of cells to different concentrations of drug for
23
24 477 24 hours (Figure 9).
25
26

27
28 478 [Figure 9 near here]
29
30

31 479 As the concentration of EGCG was increased from 0.1 to 100 μM , HDFa cell viability
32
33 480 decreased (Figure 9A) with statistical significance ($P \leq 0.0001$). This may be due to toxicity
34
35 481 or death of damaged cells in which EGCG induced apoptosis [79, 80]. Whilst limited data
36
37 482 exists on the cytotoxicity of EGCG towards dermal tissues, a study observing growth
38
39 483 inhibition in multiple cell lines, observed that EGCG at 40 μM had little or no inhibitory
40
41 484 effect on the growth of WI38 cells, normal human fibroblast cells [81]. Cell viability was
42
43 485 maintained across the concentration range of 0.1–100 μM on HaCat cells (Figure 9B). No
44
45 486 statistically significant difference was observed in cell viability ($P \geq 0.05$). Furthermore,
46
47 487 EGCG has been reported to impart protective effects in HaCat cells exposed to external
48
49 488 stressors including UVA and UVB radiation [82, 83]. Whilst some of our formulations
50
51 489 exceeded this concentration of EGCG as a whole, the retarded release profile of the
52
53
54
55
56
57
58
59
60

1
2
3 490 liposomes would be expected to result in an overall lower temporal concentration profile
4
5 491 exposure to these cells, significantly below 100 μ M.
6
7

8 492 ***3.6 Cellular liposomal uptake assay into HDFa and HaCat cells***

9
10
11 493 A primary goal for our studies was to demonstrate uptake of deformable liposomes
12
13 494 loaded with EGCG into a cell culture skin model. EGCG loaded liposomes were incubated
14
15 495 with both HaCat (Figure 10) and HDFa (Figure 11) cells to assess the cellular uptake of these
16
17 496 formulations. Liposomes formulated with 2% w/w Tween 20 were selected, a result of the
18
19 497 highest EGCG entrapment compared with the other surfactant loadings. DiIc labelled
20
21 498 liposomes loaded with EGCG incubated for 2-hours with both HaCat and HDFa cells seeded
22
23 499 onto collagen-coated coverslips and the cellular localisation of these liposomes was
24
25 500 determined using confocal microscopy. Following a 2-hour incubation with the cells,
26
27 501 intracellular localisation of labelled liposomes were clearly evident, confirming the
28
29 502 successful uptake into both HaCat and HDFa cells.
30
31

32
33
34 503 [Figure 10 and 11 near here]
35
36

37 504 Extraneous particle cell uptake is dependent upon influences such as particle size,
38
39 505 charge, affinity etc. [84-86]. There are four proposed methods of liposome uptake into cells:
40
41 506 stable adsorption, endocytosis, fusion of the lipid bilayer with the cell plasma membrane and
42
43 507 lipid transfer [43, 87]. It is unclear which of these occurred in this study, however, these
44
45 508 methods of uptake are not mutually exclusive and any combination may occur in a given
46
47 509 experimental circumstance [43]. The interaction of nanoparticles with cell membrane seems
48
49 510 to be most affected by particle surface charge. The cell membrane surface is dominated by
50
51 511 negatively charged sulphated proteoglycans molecules (vital in cellular proliferation and
52
53 512 migration) [88, 89]. These molecules are associated with glycosaminoglycan side chains
54
55 513 (heparan, dermatan, keratan or chondrotine sulfates) which are anionic, and interaction
56
57
58
59
60

1
2
3 514 between proteoglycans and liposomes, if positively charged, tend to be largely ionic [90]. The
4
5 515 liposomes applied to the cells in this study had a ζ of 3.67 ± 0.91 suggesting an ionic
6
7 516 interaction may have occurred. A study applying cationic liposomes formulated with the
8
9 517 cationic lipids Lipofectin, Tfx-50, and Lipofectamine in oligonucleotide delivery to HaCat
10
11 518 cells observed liposome uptake within 24 hours [91]. Furthermore, research developing
12
13 519 chemotherapy against malignant melanoma using mouse B16 melanoma cells as well as
14
15 520 Normal Human Dermal Fibroblasts observed a greater uptake of cationic liposomes by cells
16
17 521 in the injection site compared with neutral liposomes due to the electrostatic interaction with
18
19 522 the negative-charged phospholipid membrane of cells [92].
20
21
22

23 523 It should be noted that the confocal microscopy studies demonstrated the possibility of the
24
25 524 delivery of deformable liposomes to relevant dermal tissues using *in-vitro* cell culture
26
27 525 techniques. However, the application of such formulations could also be assessed using *ex-*
28
29 526 *vivo* human or animal dermal tissues. The ultimate aim of this delivery system was to
30
31 527 improve dermal cell uptake and delivery a controlled release of active agent, thus from a
32
33 528 regulatory perspective, pharmacokinetic data is not required as drug is not intended to reach
34
35 529 the blood stream [93].
36
37
38

39 530 In order to ascertain the extent of carrier and drug permeation a skin strip test may be
40
41 531 appropriate [70]. This involves the use of an adhesive tape to strip the skin layer by layer and
42
43 532 quantifying lipid and drug on each layer[94]. Further, whilst the most appropriate animal
44
45 533 model for human skin is the porcine skin tissue, sample-to-sample variability in addition to
46
47 534 differences in the lipid dermal matrices often results in an altered permeability profile
48
49 535 limiting the wider human translational goals [95-97].
50
51
52

53 536 **4. Conclusion**

54
55
56
57
58
59
60

1
2
3 537 Skin cancer is emerging as an increasing public health problem particularly in
4
5 538 developed countries. Current treatments include surgery to remove the tumour as well as
6
7 539 topical formulations. Such treatments may not be suitable for all patients as they are
8
9 540 associated with an unpleasant aesthetic profile as well as side effects. A nanoparticle delivery
10
11 541 system such as deformable liposomes applied topically for the direct dermal delivery of
12
13 542 compounds would be valuable in carrying compounds across the stratum corneum at a
14
15 543 controlled rate whilst limiting side effects. The use of naturally occurring compounds such as
16
17 544 EGCG have been found to be successful as chemopreventative and chemoprotective agents.
18
19 545 However, formulation of such compounds has been limited in success due to a limited
20
21 546 bioavailability of promising agents and inefficient delivery systems. We developed a novel
22
23 547 deformable liposome formulation loaded with EGCG and systemically investigated the
24
25 548 loading, uptake and *in-vitro* release of EGCG from these nanoparticles. This study has found
26
27 549 deformable liposomes could be valuable in enhancing the bioavailability of these compounds
28
29 550 as well as offering controlled release of the compound [13, 98]. We have demonstrated that
30
31 551 as the amount of Tween 20 in the liposomal bilayer is increased, liposome size decreased and
32
33 552 elasticity increased. As the loading of Tween 20 in the liposome was increased the EGCG
34
35 553 encapsulation decreased. This may have been due to Tween 20 competing for space within
36
37 554 the bilayer or due to Tween 20 increasing the solubilisation capacity of EGCG. Additionally
38
39 555 EGCG release from liposomes found that the liposomes were able to modify the release of
40
41 556 drug with complete release observed within 24 hours. Further, our studies demonstrated these
42
43 557 liposomes were capable of uptake into epidermal keratinocytes and dermal fibroblasts within
44
45 558 2 hours. This present study demonstrates liposomes formulated with Tween 20 are useful in
46
47 559 enhancing drug penetration into dermal cells and in the development of a controlled release
48
49 560 formulation crucial in improving patient compliance thus skin cancer treatment outcomes.
50
51
52
53

54
55
56 561 **Disclosure of interest**
57

1
2
3 562 The authors report no conflict of interest.
4
5

6 563 **References**
7

8
9 564 1. Lomas A, Leonardi-Bee J, Bath-Hextall F. A systematic review of worldwide incidence of
10 565 nonmelanoma skin cancer. *The British journal of dermatology*. 2012;166(5):1069-80.
11
12 566 doi:10.1111/j.1365-2133.2012.10830.x.

13
14
15 567 2. World Health Organisation. Ultraviolet radiation (UV): Skin cancers. 2017.
16
17 568 <http://www.who.int/uv/faq/skincancer/en/index1.html>. Accessed 20/11/2017 2017.

18
19 569 3. Diepgen TL, Mahler V. The epidemiology of skin cancer. *The British journal of*
20 570 *dermatology*. 2002;146 Suppl 61(s61):1-6.

21
22
23 571 4. Donaldson MR, Coldiron BM, editors. No end in sight: the skin cancer epidemic
24 572 continues. *Seminars in cutaneous medicine and surgery*; 2011: Frontline Medical
25
26 573 Communications.

27
28
29 574 5. American Cancer Society. Cancer Facts and Figures. 2017.
30 575 [http://www.cancer.org/acs/groups/content/@editorial/documents/document/acspc-](http://www.cancer.org/acs/groups/content/@editorial/documents/document/acspc-048738.pdf)
31
32 576 [048738.pdf](http://www.cancer.org/acs/groups/content/@editorial/documents/document/acspc-048738.pdf). Accessed 10/01/2017 2017.

33
34
35 577 6. Ali SM, Brodell RT, Balkrishnan R, Feldman SR. Poor adherence to treatments: A
36 578 fundamental principle of dermatology. *Archives of dermatology*. 2007;143(7):912-5.
37 579 doi:10.1001/archderm.143.7.912.

38
39 580 7. Felicio L, Ferreira J, Kurachi C, Bentley M, Tedesco A, Bagnato V. Long-term follow-up
40 581 of topical 5-aminolaevulinic acid photodynamic therapy diode laser single session for non-
41 582 melanoma skin cancer. *Photodiagnosis and photodynamic therapy*. 2009;6:207-13.

42
43
44 583 8. Kaplan B, Moy RL. Effect of perilesional injections of PEG-interleukin-2 on basal cell
45 584 carcinoma. *Dermatol Surg*. 2000;26(11):1037-40.

- 1
2
3 585 9. Neville JA, Welch E, Leffell DJ. Management of nonmelanoma skin cancer in 2007. *Nat*
4
5 586 *Clin Prac Oncol.* 2007;4(8):462-9.
6
7 587 10. Bansal T, Jaggi M, Khar R, Talegaonkar S. Emerging significance of flavonoids as P-
8
9 588 glycoprotein inhibitors in cancer chemotherapy. *Journal of Pharmacy & Pharmaceutical*
10
11 589 *Sciences.* 2009;12(1):46-78.
12
13 590 11. Kanadaswami C, Lee L-T, Lee P-PH, Hwang J-J, Ke F-C, Huang Y-T et al. The
14
15 591 antitumor activities of flavonoids. *In Vivo.* 2005;19(5):895-909.
16
17 592 12. Carey MP, Burish TG. Etiology and treatment of the psychological side effects associated
18
19 593 with cancer chemotherapy: A critical review and discussion. *Psychological bulletin.*
20
21 594 1988;104(3):307.
22
23 595 13. Siddiqui IA, Adhami VM, Bharali DJ, Hafeez BB, Asim M, Khwaja SI et al. Introducing
24
25 596 Nanochemoprevention as a Novel Approach for Cancer Control: Proof of Principle with
26
27 597 Green Tea Polyphenol Epigallocatechin-3-Gallate. *Cancer research.* 2009;69(5):1712-6.
28
29 598 doi:10.1158/0008-5472.can-08-3978.
30
31 599 14. Hwang J-T, Ha J, Park I-J, Lee S-K, Baik HW, Kim YM et al. Apoptotic effect of EGCG
32
33 600 in HT-29 colon cancer cells via AMPK signal pathway. *Cancer letters.* 2007;247(1):115-21.
34
35 601 doi:<http://dx.doi.org/10.1016/j.canlet.2006.03.030>.
36
37 602 15. Singh BN, Shankar S, Srivastava RK. Green tea catechin, epigallocatechin-3-gallate
38
39 603 (EGCG): Mechanisms, perspectives and clinical applications. *Biochemical pharmacology.*
40
41 604 2011;82(12):1807-21. doi:<http://dx.doi.org/10.1016/j.bcp.2011.07.093>.
42
43 605 16. Casey SC, Amedei A, Aquilano K, Azmi AS, Benencia F, Bhakta D et al. Cancer
44
45 606 prevention and therapy through the modulation of the tumor microenvironment. *Seminars in*
46
47 607 *cancer biology.* 2015. doi:10.1016/j.semcancer.2015.02.007.
48
49
50
51
52
53
54
55
56
57
58
59
60

- 1
2
3 608 17. Gupta S, Hastak K, Afaq F, Ahmad N, Mukhtar H. Essential role of caspases in
4
5 609 epigallocatechin-3-gallate-mediated inhibition of nuclear factor kappa B and induction of
6
7 610 apoptosis. *Oncogene*. 2004;23(14):2507-22. doi:10.1038/sj.onc.1207353.
8
9 611 18. Singh T, Vaid M, Katiyar N, Sharma S, Katiyar SK. Berberine, an isoquinoline alkaloid,
10
11 612 inhibits melanoma cancer cell migration by reducing the expressions of cyclooxygenase-2,
12
13 613 prostaglandin E(2) and prostaglandin E(2) receptors. *Carcinogenesis*. 2011;32(1):86-92.
14
15 614 doi:10.1093/carcin/bgq215.
16
17 615 19. Thawonsuwan J, Kiron V, Satoh S, Panigrahi A, Verlhac V. Epigallocatechin-3-gallate
18
19 616 (EGCG) affects the antioxidant and immune defense of the rainbow trout, *Oncorhynchus*
20
21 617 *mykiss*. *Fish physiology and biochemistry*. 2010;36(3):687-97. doi:10.1007/s10695-009-
22
23 618 9344-4.
24
25 619 20. Sigler K, Ruch RJ. Enhancement of gap junctional intercellular communication in tumor
26
27 620 promoter-treated cells by components of green tea. *Cancer letters*. 1993;69(1):15-9.
28
29 621 21. Basnet P, Hussain H, Tho I, Skalko-Basnet N. Liposomal delivery system enhances anti-
30
31 622 inflammatory properties of curcumin. *J Pharm Sci*. 2012;101(2):598-609.
32
33 623 doi:10.1002/jps.22785.
34
35 624 22. Wang Y, Wang S, Firempong CK, Zhang H, Wang M, Zhang Y et al. Enhanced
36
37 625 Solubility and Bioavailability of Naringenin via Liposomal Nanoformulation: Preparation
38
39 626 and In Vitro and In Vivo Evaluations. *Aaps Pharmscitech*. 2016. doi:10.1208/s12249-016-
40
41 627 0537-8.
42
43 628 23. Zhao Y-Z, Lu C-T, Zhang Y, Xiao J, Zhao Y-P, Tian J-L et al. Selection of high efficient
44
45 629 transdermal lipid vesicle for curcumin skin delivery. *Int J Pharmaceut*. 2013;454(1):302-9.
46
47 630 24. Alexander A, Dwivedi S, Giri TK, Saraf S, Saraf S, Tripathi DK. Approaches for
48
49 631 breaking the barriers of drug permeation through transdermal drug delivery. *J Control*
50
51 632 *Release*. 2012;164(1):26-40.
52
53
54
55
56
57
58
59
60

- 1
2
3 633 25. Lopez RF, Seto JE, Blankschtein D, Langer R. Enhancing the transdermal delivery of
4
5 634 rigid nanoparticles using the simultaneous application of ultrasound and sodium lauryl
6
7 635 sulfate. *Biomaterials*. 2011;32(3):933-41. doi:10.1016/j.biomaterials.2010.09.060.
8
9 636 26. Tsai MJ, Huang YB, Fang JW, Fu YS, Wu PC. Preparation and Characterization of
10
11 637 Naringenin-Loaded Elastic Liposomes for Topical Application. *PloS one*.
12
13 638 2015;10(7):e0131026. doi:10.1371/journal.pone.0131026.
14
15 639 27. Alexander A, Dwivedi S, Ajazuddin, Giri TK, Saraf S, Saraf S et al. Approaches for
16
17 640 breaking the barriers of drug permeation through transdermal drug delivery. *J Control*
18
19 641 *Release*. 2012;164(1):26-40. doi:DOI 10.1016/j.jconrel.2012.09.017.
20
21 642 28. Bouwstra JA, Honeywell-Nguyen PL. Skin structure and mode of action of vesicles. *Adv*
22
23 643 *Drug Deliv Rev*. 2002;54 Suppl 1:S41-55.
24
25 644 29. du Plessis J, Weiner N, Müller D. The influence of in vivo treatment of skin with
26
27 645 liposomes on the topical absorption of a hydrophilic and a hydrophobic drug in vitro. *Int J*
28
29 646 *Pharmaceut*. 1994;103(2):R1-R5.
30
31 647 30. Park S-I, Lee E-O, Yang H-M, Park CW, Kim J-D. Polymer-hybridized liposomes of
32
33 648 poly (amino acid) derivatives as transepidermal carriers. *Colloids and Surfaces B:*
34
35 649 *Biointerfaces*. 2013;110:333-8.
36
37 650 31. Cevc G, Gebauer D, Stieber J, Schätzlein A, Blume G. Ultraflexible vesicles,
38
39 651 Transfersomes, have an extremely low pore penetration resistance and transport therapeutic
40
41 652 amounts of insulin across the intact mammalian skin. *Biochimica et Biophysica Acta (BBA) -*
42
43 653 *Biomembranes*. 1998;1368(2):201-15. doi:[http://dx.doi.org/10.1016/S0005-2736\(97\)00177-](http://dx.doi.org/10.1016/S0005-2736(97)00177-6)
44
45 654 [6](http://dx.doi.org/10.1016/S0005-2736(97)00177-6).
46
47 655 32. Goindi S, Kumar G, Kumar N, Kaur A. Development of novel elastic vesicle-based
48
49 656 topical formulation of cetirizine dihydrochloride for treatment of atopic dermatitis. *Aaps*
50
51 657 *Pharmscitech*. 2013;14(4):1284-93. doi:10.1208/s12249-013-0017-3.
52
53
54
55
56
57
58
59
60

- 1
2
3 658 33. El MGMM, C. WA, W. BB. Skin delivery of 5-fluorouracil from ultradeformable and
4
5 659 standard liposomes in-vitro. J Pharm Pharmacol. 2001;53(8):1069-77.
6
7 660 doi:doi:10.1211/0022357011776450.
8
9 661 34. Cevc GS, A.; Gebauer, D.; Blume, G. Ultra-high efficiency of drug and peptide transfer
10
11 662 through the intact skin by means of novel drug-carriers, Transfersomes. In: Bain KRH, J.;
12
13 663 James, W.J.; Water, K.A., editor. Prediction of Percutaneous Penetration. Cardiff: STS
14
15 664 Publishing; 1993. p. 226-34.
16
17 665 35. Cevc G, Schätzlein A, Gebauer D, Blume G. Ultra-high efficiency of drugs and peptide
18
19 666 transfer through the intact skin by means of novel drug carriers, transfersomes. STS
20
21 667 Publishing; 1993.
22
23 668 36. Cevc G. Material transport across permeability barriers by means of lipid vesicles.
24
25 669 Handbook of biological physics. 1995;1:465-90.
26
27 670 37. Romero EL, Morilla MJ. Highly deformable and highly fluid vesicles as potential drug
28
29 671 delivery systems: theoretical and practical considerations. Int J Nanomedicine. 2013;8:3171-
30
31 672 86. doi:10.2147/ijn.s33048.
32
33 673 38. Oh YK, Kim MY, Shin JY, Kim TW, Yun MO, Yang SJ et al. Skin permeation of retinol
34
35 674 in Tween 20-based deformable liposomes: in-vitro evaluation in human skin and keratinocyte
36
37 675 models. J Pharm Pharmacol. 2006;58(2):161-6. doi:10.1211/jpp.58.2.0002.
38
39 676 39. Cevc G. Transfersomes, liposomes and other lipid suspensions on the skin: permeation
40
41 677 enhancement, vesicle penetration, and transdermal drug delivery. Crit Rev Ther Drug Carrier
42
43 678 Syst. 1996;13(3-4):257-388.
44
45 679 40. Ita KB, Du Preez J, Lane ME, Hadgraft J, du Plessis J. Dermal delivery of selected
46
47 680 hydrophilic drugs from elastic liposomes: effect of phospholipid formulation and surfactants.
48
49 681 J Pharm Pharmacol. 2007;59(9):1215-22. doi:10.1211/jpp.59.9.0005.
50
51
52
53
54
55
56
57
58
59
60

- 1
2
3 682 41. Bangham AD, Standish MM, Watkins JC. Diffusion of univalent ions across the lamellae
4
5 683 of swollen phospholipids. *Journal of molecular biology*. 1965;13(1):238-52.
6
7 684 42. Hiruta Y, Hattori Y, Kawano K, Obata Y, Maitani Y. Novel ultra-deformable vesicles
8
9 685 entrapped with bleomycin and enhanced to penetrate rat skin. *J Control Release*.
10
11 686 2006;113(2):146-54. doi:<http://dx.doi.org/10.1016/j.jconrel.2006.04.016>.
12
13 687 43. Pagano RE, Weinstein JN. Interactions of liposomes with mammalian cells. *Annual*
14
15 688 *review of biophysics and bioengineering*. 1978;7(1):435-68.
16
17 689 44. Ali MH, Moghaddam B, Kirby DJ, Mohammed AR, Perrie Y. The role of lipid geometry
18
19 690 in designing liposomes for the solubilisation of poorly water soluble drugs. *Int J Pharmaceut*.
20
21 691 2013;453(1):225-32. doi:DOI 10.1016/j.ijpharm.2012.06.056.
22
23 692 45. Lasic DD, Barenholz Y. *Handbook of nonmedical applications of liposomes: Theory and*
24
25 693 *basic sciences*. CRC Press; 1996.
26
27 694 46. Song Y-K, Kim C-K. Topical delivery of low-molecular-weight heparin with surface-
28
29 695 charged flexible liposomes. *Biomaterials*. 2006;27(2):271-80.
30
31 696 doi:<http://dx.doi.org/10.1016/j.biomaterials.2005.05.097>.
32
33 697 47. Bradfield A, Penney M. 456. The catechins of green tea. Part II. *Journal of the Chemical*
34
35 698 *Society (Resumed)*. 1948:2249-54.
36
37 699 48. Korsmeyer RW, Gurny R, Doelker E, Buri P, Peppas NA. Mechanisms of solute release
38
39 700 from porous hydrophilic polymers. *Int J Pharmaceut*. 1983;15(1):25-35.
40
41 701 doi:[http://dx.doi.org/10.1016/0378-5173\(83\)90064-9](http://dx.doi.org/10.1016/0378-5173(83)90064-9).
42
43 702 49. Scudiero DA, Shoemaker RH, Paull KD, Monks A, Tierney S, Nofziger TH et al.
44
45 703 Evaluation of a soluble tetrazolium/formazan assay for cell growth and drug sensitivity in
46
47 704 culture using human and other tumor cell lines. *Cancer research*. 1988;48(17):4827-33.
48
49
50
51
52
53
54
55
56
57
58
59
60

- 1
2
3 705 50. Yang CS, Maliakal P, Meng X. Inhibition of carcinogenesis by tea. Annual review of
4
5 706 pharmacology and toxicology. 2002;42:25-54.
6
7 707 doi:10.1146/annurev.pharmtox.42.082101.154309.
8
9 708 51. McLoughlin P, Roengvoraphoj M, Gissel C, Hescheler J, Certa U, Sachinidis A.
10
11 709 Transcriptional responses to epigallocatechin-3 gallate in HT 29 colon carcinoma spheroids.
12
13 710 Genes to cells : devoted to molecular & cellular mechanisms. 2004;9(7):661-9.
14
15 711 doi:10.1111/j.1356-9597.2004.00754.x.
16
17 712 52. El Zaafarany GM, Awad GA, Holayel SM, Mortada ND. Role of edge activators and
18
19 713 surface charge in developing ultradeformable vesicles with enhanced skin delivery. Int J
20
21 714 Pharmaceut. 2010;397(1):164-72.
22
23
24 715 53. Chen Y, Wu Q, Zhang Z, Yuan L, Liu X, Zhou L. Preparation of curcumin-loaded
25
26 716 liposomes and evaluation of their skin permeation and pharmacodynamics. Molecules.
27
28 717 2012;17(5):5972-87. doi:10.3390/molecules17055972.
29
30 718 54. Kang SN, Hong S-S, Kim S-Y, Oh H, Lee M-K, Lim S-J. Enhancement of liposomal
31
32 719 stability and cellular drug uptake by incorporating tributyrin into celecoxib-loaded liposomes.
33
34 720 Asian Journal of Pharmaceutical Sciences. 2013;8(2):128-33.
35
36 721 doi:<http://dx.doi.org/10.1016/j.ajps.2013.07.016>.
37
38
39 722 55. Prausnitz MR, Langer R. Transdermal drug delivery. Nat Biotech. 2008;26(11):1261-8.
40
41 723 56. Weiner N, Egbaria K, Ramachandran C. Topical Delivery of Liposomally Encapsulated
42
43 724 Interferon Evaluated by In Vitro Diffusion Studies and in a Cutaneous Herpes Guinea Pig
44
45 725 Model. In: Braun-Falco O, Korting HC, Maibach HI, editors. Liposome Dermatics:
46
47 726 Griesbach Conference. Berlin, Heidelberg: Springer Berlin Heidelberg; 1992. p. 242-50.
48
49 727 57. El Maghraby GMM, Williams AC, Barry BW. Oestradiol skin delivery from
50
51 728 ultradeformable liposomes: refinement of surfactant concentration. Int J Pharmaceut.
52
53 729 2000;196(1):63-74. doi:[http://dx.doi.org/10.1016/S0378-5173\(99\)00441-X](http://dx.doi.org/10.1016/S0378-5173(99)00441-X).
54
55
56
57
58
59
60

- 1
2
3 730 58. Levy MY, Benita S, Baszkin A. Interactions of a non-ionic surfactant with mixed
4
5 731 phospholipid—oleic acid monolayers. Studies under dynamic conditions. Colloid Surface.
6
7 732 1991;59:225-41. doi:[http://dx.doi.org/10.1016/0166-6622\(91\)80249-N](http://dx.doi.org/10.1016/0166-6622(91)80249-N).
8
9 733 59. Casas M, Baszkin A. Interactions of a non-ionic surfactant with mixed phospholipid—
10
11 734 oleic acid monolayers. Surface potential and surface pressure studies at constant area. Colloid
12
13 735 Surface. 1992;63(3):301-9. doi:[http://dx.doi.org/10.1016/0166-6622\(92\)80252-W](http://dx.doi.org/10.1016/0166-6622(92)80252-W).
14
15 736 60. Almog S, Kushnir T, Nir S, Lichtenberg D. Kinetic and structural aspects of
16
17 737 reconstitution of phosphatidylcholine vesicles by dilution of phosphatidylcholine-sodium
18
19 738 cholate mixed micelles. Biochemistry. 1986;25(9):2597-605.
20
21 739 61. Almog S, Kushnir T, Nir S, Lichtenberg D. Kinetic and structural aspects of
22
23 740 reconstitution of phosphatidylcholine vesicles by dilution of phosphatidylcholine-sodium
24
25 741 cholate mixed micelles. Biochemistry. 1986;25(9):2597-605.
26
27 742 62. Trotta M, Peira E, Carlotti ME, Gallarate M. Deformable liposomes for dermal
28
29 743 administration of methotrexate. Int J Pharm. 2004;270(1-2):119-25.
30
31 744 63. Fresta M, Puglisi G. Application of liposomes as potential cutaneous drug delivery
32
33 745 systems. In vitro and in vivo investigation with radioactively labelled vesicles. J Drug Target.
34
35 746 1996;4(2):95-101. doi:10.3109/10611869609046267.
36
37 747 64. Gompper G, Kroll DM. Driven transport of fluid vesicles through narrow pores. Physical
38
39 748 review E, Statistical physics, plasmas, fluids, and related interdisciplinary topics.
40
41 749 1995;52(4):4198-208.
42
43 750 65. Trotta M, Peira E, Debernardi F, Gallarate M. Elastic liposomes for skin delivery of
44
45 751 dipotassium glycyrrhizinate. Int J Pharmaceut. 2002;241(2):319-27.
46
47 752 doi:[http://dx.doi.org/10.1016/S0378-5173\(02\)00266-1](http://dx.doi.org/10.1016/S0378-5173(02)00266-1).
48
49 753 66. Chung H, Caffrey M. The curvature elastic-energy function of the lipid-water cubic
50
51 754 mesophase. Nature. 1994;368(6468):224-6. doi:10.1038/368224a0.
52
53
54
55
56
57
58
59
60

- 1
2
3 755 67. Vajjha RS, Das DK, Kulkarni DP. Development of new correlations for convective heat
4
5 756 transfer and friction factor in turbulent regime for nanofluids. *International Journal of Heat*
6
7 757 and *Mass Transfer*. 2010;53(21):4607-18.
8
9 758 doi:<http://dx.doi.org/10.1016/j.ijheatmasstransfer.2010.06.032>.
- 10
11 759 68. Kirjavainen M, Urtti A, Jääskeläinen I, Marjukka Suhonen T, Paronen P, Valjakka-
12
13 760 Koskela R et al. Interaction of liposomes with human skin in vitro — The influence of lipid
14
15 761 composition and structure. *Biochimica et Biophysica Acta (BBA) - Lipids and Lipid*
16
17 762 *Metabolism*. 1996;1304(3):179-89. doi:[http://dx.doi.org/10.1016/S0005-2760\(96\)00126-9](http://dx.doi.org/10.1016/S0005-2760(96)00126-9).
- 18
19 763 69. El Maghraby GM, Barry BW, Williams AC. Liposomes and skin: From drug delivery to
20
21 764 model membranes. *Eur J Pharm Sci*. 2008;34(4-5):203-22.
22
23 765 doi:<http://dx.doi.org/10.1016/j.ejps.2008.05.002>.
- 24
25 766 70. Schäfer-Korting M, Mehnert W, Korting H-C. Lipid nanoparticles for improved topical
26
27 767 application of drugs for skin diseases. *Adv Drug Deliver Rev*. 2007;59(6):427-43.
28
29 768 doi:<http://dx.doi.org/10.1016/j.addr.2007.04.006>.
- 30
31 769 71. Guy RH, Hadgraft J. Transdermal drug delivery: a simplified pharmacokinetic approach.
32
33 770 *Int J Pharmaceut*. 1985;24(2-3):267-74.
- 34
35 771 72. Cho HH, Han D-W, Matsumura K, Tsutsumi S, Hyon S-H. The behavior of vascular
36
37 772 smooth muscle cells and platelets onto epigallocatechin gallate-releasing poly(l-lactide-co-ε-
38
39 773 caprolactone) as stent-coating materials. *Biomaterials*. 2008;29(7):884-93.
40
41 774 doi:<http://dx.doi.org/10.1016/j.biomaterials.2007.10.052>.
- 42
43 775 73. Chu KA, Yalkowsky SH. An interesting relationship between drug absorption and
44
45 776 melting point. *Int J Pharm*. 2009;373(1-2):24-40. doi:10.1016/j.ijpharm.2009.01.026.
- 46
47 777 74. Neslihan Gursoy R, Benita S. Self-emulsifying drug delivery systems (SEDDS) for
48
49 778 improved oral delivery of lipophilic drugs. *Biomedicine & Pharmacotherapy*.
50
51 779 2004;58(3):173-82. doi:<https://doi.org/10.1016/j.biopha.2004.02.001>.
- 52
53
54
55
56
57
58
59
60

- 1
2
3 780 75. Vasconcelos T, Sarmiento B, Costa P. Solid dispersions as strategy to improve oral
4
5 781 bioavailability of poor water soluble drugs. *Drug discovery today*. 2007;12(23):1068-75.
6
7 782 doi:<https://doi.org/10.1016/j.drudis.2007.09.005>.
8
9 783 76. Peppas NA, Sahlin JJ. A simple equation for the description of solute release. III.
10
11 784 Coupling of diffusion and relaxation. *Int J Pharmaceut*. 1989;57(2):169-72.
12
13 785 doi:[http://dx.doi.org/10.1016/0378-5173\(89\)90306-2](http://dx.doi.org/10.1016/0378-5173(89)90306-2).
14
15 786 77. Lentz BR, Carpenter TJ, Alford DR. Spontaneous fusion of phosphatidylcholine small
16
17 787 unilamellar vesicles in the fluid phase. *Biochemistry*. 1987;26(17):5389-97.
18
19 788 78. Seras M, Handjani-Vila R-M, Ollivon M, Lesieur S. Kinetic aspects of the solubilization
20
21 789 of non-ionic monoalkyl amphiphile-cholesterol vesicles by octylglucoside. *Chem Phys*
22
23 790 *Lipids*. 1992;63(1-2):1-14. doi:[http://dx.doi.org/10.1016/0009-3084\(92\)90015-H](http://dx.doi.org/10.1016/0009-3084(92)90015-H).
24
25 791 79. Bae JY, Choi JS, Choi YJ, Shin SY, Kang SW, Han SJ et al. (-)Epigallocatechin gallate
26
27 792 hampers collagen destruction and collagenase activation in ultraviolet-B-irradiated human
28
29 793 dermal fibroblasts: involvement of mitogen-activated protein kinase. *Food and chemical*
30
31 794 *toxicology : an international journal published for the British Industrial Biological Research*
32
33 795 *Association*. 2008;46(4):1298-307. doi:10.1016/j.fct.2007.09.112.
34
35 796 80. Tanigawa T, Kanazawa S, Ichibori R, Fujiwara T, Magome T, Shingaki K et al. (+)-
36
37 797 Catechin protects dermal fibroblasts against oxidative stress-induced apoptosis. *BMC*
38
39 798 *complementary and alternative medicine*. 2014;14:133. doi:10.1186/1472-6882-14-133.
40
41 799 81. Chen ZP, Schell JB, Ho C-T, Chen KY. Green tea epigallocatechin gallate shows a
42
43 800 pronounced growth inhibitory effect on cancerous cells but not on their normal counterparts.
44
45 801 *Cancer letters*. 1998;129(2):173-9. doi:[http://dx.doi.org/10.1016/S0304-3835\(98\)00108-6](http://dx.doi.org/10.1016/S0304-3835(98)00108-6).
46
47 802 82. Huang C-C, Fang J-Y, Wu W-B, Chiang H-S, Wei Y-J, Hung C-F. Protective effects of
48
49 803 (-)-epicatechin-3-gallate on UVA-induced damage in HaCaT keratinocytes. *Archives of*
50
51 804 *dermatological research*. 2005;296(10):473-81.
52
53
54
55
56
57
58
59
60

- 1
2
3 805 83. Huang C-C, Wu W-B, Fang J-Y, Chiang H-S, Chen S-K, Chen B-H et al. (-)-Epicatechin-
4
5 806 3-gallate, a green tea polyphenol is a potent agent against UVB-induced damage in HaCaT
6
7 807 keratinocytes. *Molecules*. 2007;12(8):1845-58.
8
9 808 84. Patil S, Sandberg A, Heckert E, Self W, Seal S. Protein adsorption and cellular uptake of
10
11 809 cerium oxide nanoparticles as a function of zeta potential. *Biomaterials*. 2007;28(31):4600-7.
12
13 810 doi:10.1016/j.biomaterials.2007.07.029.
14
15 811 85. Chen C-C, Tsai T-H, Huang Z-R, Fang J-Y. Effects of lipophilic emulsifiers on the oral
16
17 812 administration of lovastatin from nanostructured lipid carriers: Physicochemical
18
19 813 characterization and pharmacokinetics. *Eur J Pharm Biopharm*. 2010;74(3):474-82.
20
21 814 doi:<https://doi.org/10.1016/j.ejpb.2009.12.008>.
22
23 815 86. Kyung OY, Grabinski CM, Schrand AM, Murdock RC, Wang W, Gu B et al. Toxicity of
24
25 816 amorphous silica nanoparticles in mouse keratinocytes. *Journal of Nanoparticle Research*.
26
27 817 2009;11(1):15-24.
28
29 818 87. Martin FJ, MacDonald RC. Lipid vesicle-cell interactions. I. Hemagglutination and
30
31 819 hemolysis. *The Journal of cell biology*. 1976;70(3):494-505.
32
33 820 88. Merton Bernfield, Martin Götte, Pyong Woo Park, Ofer Reizes, Marilyn L. Fitzgerald,
34
35 821 John Lincecum a et al. Functions of Cell Surface Heparan Sulfate Proteoglycans. *Annual*
36
37 822 *Review of Biochemistry*. 1999;68(1):729-77. doi:10.1146/annurev.biochem.68.1.729.
38
39 823 89. Mislick KA, Baldeschwieler JD. Evidence for the role of proteoglycans in cation-
40
41 824 mediated gene transfer. *Proceedings of the National Academy of Sciences*.
42
43 825 1996;93(22):12349-54.
44
45 826 90. Panyam J, Labhasetwar V. Biodegradable nanoparticles for drug and gene delivery to
46
47 827 cells and tissue. *Adv Drug Deliv Rev*. 2003;55(3):329-47.
48
49 828 91. White PJ, Fogarty RD, McKean SC, Venables DJ, Werther GA, Wraight CJ.
50
51 829 Oligonucleotide Uptake in Cultured Keratinocytes: Influence of Confluence, Cationic
52
53
54
55
56
57
58
59
60

- 1
2
3 830 Liposomes, and Keratinocyte Cell Type. *J Invest Dermatol.* 1999;112(5):699-705.
4
5 831 doi:<https://doi.org/10.1046/j.1523-1747.1999.00578.x>.
6
7 832 92. Ito A, Fujioka M, Yoshida T, Wakamatsu K, Ito S, Yamashita T et al. 4-S-
8
9 833 Cysteaminyphenol-loaded magnetite cationic liposomes for combination therapy of
10
11 834 hyperthermia with chemotherapy against malignant melanoma. *Cancer science.*
12
13 835 2007;98(3):424-30. doi:10.1111/j.1349-7006.2006.00382.x.
14
15 836 93. Products EAftEoM. Note for Guidance on the Investigation of Bioavailability and
16
17 837 Bioequivalence. London: European Agency for the Evaluation of Medicinal Products
18
19
20 838 2000 14/12/2000.
21
22 839 94. Weigmann H, Lademann J, Meffert H, Schaefer H, Sterry W. Determination of the horny
23
24 840 layer profile by tape stripping in combination with optical spectroscopy in the visible range as
25
26 841 a prerequisite to quantify percutaneous absorption. *Skin Pharmacol Appl Skin Physiol.*
27
28 842 1999;12(1-2):34-45. doi:10.1159/000029844.
29
30 843 95. Schmook FP, Meingassner JG, Billich A. Comparison of human skin or epidermis models
31
32 844 with human and animal skin in in-vitro percutaneous absorption. *Int J Pharmaceut.*
33
34 845 2001;215(1-2):51-6.
35
36 846 96. Dick IP, Scott RC. Pig ear skin as an in - vitro model for human skin permeability. *J*
37
38 847 *Pharm Pharmacol.* 1992;44(8):640-5.
39
40 848 97. Godin B, Touitou E. Transdermal skin delivery: predictions for humans from in vivo, ex
41
42 849 vivo and animal models. *Adv Drug Deliver Rev.* 2007;59(11):1152-61.
43
44 850 98. Nishiyama N. Nanomedicine: Nanocarriers shape up for long life. *Nat Nano.*
45
46 851 2007;2(4):203-4.
47
48
49
50
51
52 852
53
54
55 853
56
57
58
59
60

1
2
3 854 **Table 1:** Zeta potential of liposomal formulations formulated in the absence and presence of
4
5 855 up to 10% w/w of Tween 20
6
7

Surfactant loading (% w/w)	Zeta potential (mV)	
	'empty'	EGCG loaded
	liposomes	liposomes
0	5.03 ± 1.03	2.41 ± 1.08
2	4.67 ± 1.08	3.67 ± 0.91
6	3.71 ± 0.90	-0.99 ± 1.01
10	-2.79 ± 0.20	-1.90 ± 0.88

856 Results are presented as the mean ± standard deviation (n=3)
24
25
26

27 857
28
29
30
31
32
33
34
35
36
37
38
39
40
41
42
43
44
45
46
47
48
49
50
51
52
53
54
55
56
57
58
59
60

Table 2: *In-vitro* SA release kinetics models

Kinetic model	Parameter	Tween 20 Loading (% w/w)			
		0	2	6	10
0	$(k_0) \times 10^{-2}$	1.01 ± 0.05	1.18 ± 0.01	2.75 ± 0.05	7.77 ± 0.02
	mg • min ⁻¹				
	R ²	0.95 ± 0.02	0.99 ± 0.01	0.93 ± 0.07	0.72 ± 0.30
	AIC	28.59 ± 4.44	18.82 ± 2.96	57.24 ± 14.21	98.21 ± 25.32
1st	$(k_1) \times 10^{-4}$	1.07 ± 0.05	1.27 ± 0.13	3.32 ± 0.58	15.04 ± 3.11
	min ⁻¹				
	R ²	0.96 ± 0.02	0.986 ± 0.01	0.96 ± 0.04	0.94 ± 0.06
	AIC	25.68 ± 4.40	18.132 ± 6.83	54.03 ± 6.46	4.56 ± 17.86
Higuchi	k _H	0.26 ± 0.01	0.294 ± 0.03	0.71 ± 0.09	2.12 ± 0.14
	R ²	0.83 ± 0.04	0.7513 ± 0.03	0.81 ± 0.05	0.86 ± 0.10
	AIC	47.40 ± 5.92	58.783 ± 4.90	77.32 ± 9.63	99.05 ± 13.13
Korsmeyer-Peppas	k _{KP}	0.03 ± 0.01	0.059 ± 0.08	0.09 ± 0.06	0.99 ± 1.01
	N	0.84 ± 0.07	0.913 ± 0.19	0.84 ± 0.12	0.72 ± 0.25
	R ²	0.99 ± 0.01	0.991 ± 0.01	0.99 ± 0.01	0.96 ± 0.03
	AIC	11.26 ± 3.00	27.163 ± 22.24	49.82 ± 8.49	82.76 ± 9.81

859 R², coefficient of determination; AIC, Akaike Information Criterion; F is the fraction of drug released at time t; k₀ is the zero-order release

860 constant; k₁ is the first-order release constant; k_H is the Higuchi release constant; k_{KP} is the release constant incorporating structural and

861 geometric characteristics of the drug- dosage form; n is diffusion release exponent.

862 **List of figures**

863 **Fig. 1** Liposome size distribution and polydispersity of ‘empty’ and EGCG loaded liposomes

864 Liposome size distribution and polydispersity, determined by DLS, comparing (A) ‘empty’
865 and (B) EGCG loaded formulations with Tween 20 (0-10 % w/w). Liposomes were prepared
866 by the dry film hydration method and EGCG added during the lipid mixing stage. Data
867 represents mean \pm SD. n=3 independent batches. **** indicates statistical comparison
868 between the size of liposome formulations with a $P \leq 0.0001$. # # indicates statistical
869 comparison between the polydispersity of liposome formulations with a $P \leq 0.01$.

870 **Fig. 2** Entrapment efficiency of EGCG in liposomes formulated with 0-10% w/w Tween 20

871 Entrapment efficiency (%) of EGCG in liposomes formulated with varying amounts of
872 Tween 20 (0-10% w/w) Data represents mean \pm SD. n=3 independent batches. **** indicates
873 statistical comparison between the entrapment efficiency of liposome formulations with a $P \leq$
874 0.0001.

875 **Fig. 3** Deformability index for ‘empty’ and EGCG loaded liposomes

876 Deformability index following extrusion through 50 nm membranes for ‘empty’ and EGCG
877 loaded liposomes with increasing surfactant loading up to a maximum of 10% w/w.
878 Liposomes were prepared adapting the dry film method adding the surfactant and adding
879 EGCG during the lipid mixing stage. The preparation was vortexed and then extruded though
880 the membranes. Data represents mean \pm SD. n=3 independent batches. **** indicates
881 statistical comparison between the DI of liposome formulations with a $P \leq 0.0001$.

882 **Fig. 4** Differential scanning calorimetry scan of EGCG

883 All experimental runs commenced at an initial temperature of 0 °C with a scan rate of 10
884 °C/min to 300 °C. Peak a and b are related to the epimer of EGCG, GCG. Peak c represents
885 the glass transition temperature (T_c) of EGCG was at 220 °C and the melting point (T_m) of
886 EGCG was at 245 °C.

887 **Fig. 5** Differential scanning calorimetry analysis scans of PC, cholesterol and Tween 20 and
888 EGCG blends

889 DSC analysis scans of (A) PC, cholesterol and Tween 20 blend and (B) PC, cholesterol,
890 Tween 20 and EGCG blend. The T_m of the lipid mixture is 172 °C, and upon addition of
891 EGCG, the T_m was 191 °C. All experimental runs started at an initial temperature of 0 °C,
892 purged under nitrogen gas, with a scan rate of 10 °C/min to 300 °C.

893 **Fig. 6** *In-vitro* percentage EGCG cumulative release profiles from solution and liposomal
894 formulations

895 EGCG release profiles from solution and liposomes formulated with 0, 2, 6 or 10 % w/w
896 Tween 20 over 24 hours. Liposomes were prepared adapting the dry film method adding the
897 surfactant and EGCG during the lipid mixing stage. A diffusion cell dialysis system was used
898 to evaluate *in-vitro* drug release. Data represents mean \pm SD. n=3 independent batches. ****

1
2
3 899 indicates statistical comparison between the EGCG release of liposome formulations with a P
4 900 ≤ 0.0001 .

5
6 901 **Fig. 7** Stability of EGCG loaded liposomes as determined by size

7
8 902 Size of EGCG loaded liposomes formulated with 0-10% w/w Tween 20, using DLS,
9 903 formulated with up to 10% w/w Tween 20 measured on various days (1, 7, 14, 21 and 28).
10 904 Data represents mean \pm SD. n=6 independent batches.

11
12 905 **Fig. 8** Liposome encapsulation efficiency for EGCG

13
14 906 Liposome encapsulation efficiency for EGCG in liposomes formulated with 2 % w/w Tween
15 907 20 liposomes over 28 days. Liposomes were prepared adapting the dry film method adding
16 908 the surfactant and drug during the lipid mixing stage. The preparation was then washed via
17 909 centrifugation. The quantity of EGCG in supernatant over 28 days was then analysed by
18 910 HPLC coupled with UV detection to assess liposome stability. Data represents mean \pm SD.
19 911 n=6 independent batches.

20
21 912 **Fig. 9** Cellular toxicity of EGCG

22
23 913 HDFa (A) and HaCat (B) cells were grown on a 96-well plate at a density of 50×10^3 cells
24 914 per well and exposed to various concentrations of EGCG (0.01-100 μ M) for 24 hours.
25 915 Thereafter 25 μ L of a 12.5:1 parts mixture of XTT to menadione was added each well. Plates
26 916 were incubated for 3 hours at 37°C and the absorbance read at 450 nm. Data is reported as
27 917 mean \pm SD with 6 replicates per compound in at 3 independent experiments. ****, ***, **, *
28 918 indicates statistical comparison between the entrapment efficiency of liposome formulations
29 919 with a $P \leq 0.0001$, 0.001, 0.01 and 0.05 respectively.

30
31 920 **Fig. 10** Localisation of DilC labelled liposomes loaded with EGCG and 2% w/w Tween 20 in
32 921 HaCat cells

33
34 922 Cells were grown on the coverslips for 2 days. Cell nuclei were visualised using (A) DAPI
35 923 (Blue). Liposomes were formulated with DilC for visualisation (B) (yellow). Liposome
36 924 localisation within the cell is shown in the merged image (C).

37
38 925 **Fig. 11** Localisation of DilC labelled liposomes loaded with EGCG and 2% w/w Tween 20 in
39 926 HDFa cells

40
41 927 Cells were grown on the coverslips for 2 days. Cell nuclei were visualised using (A) DAPI
42 928 (Blue). Liposomes were formulated with DilC for visualisation (B) (yellow). Liposome
43 929 localisation within the cell is shown in the merged image (C).

44
45 930

46
47
48
49 931 **Word count: 10773**

50
51
52
53 932

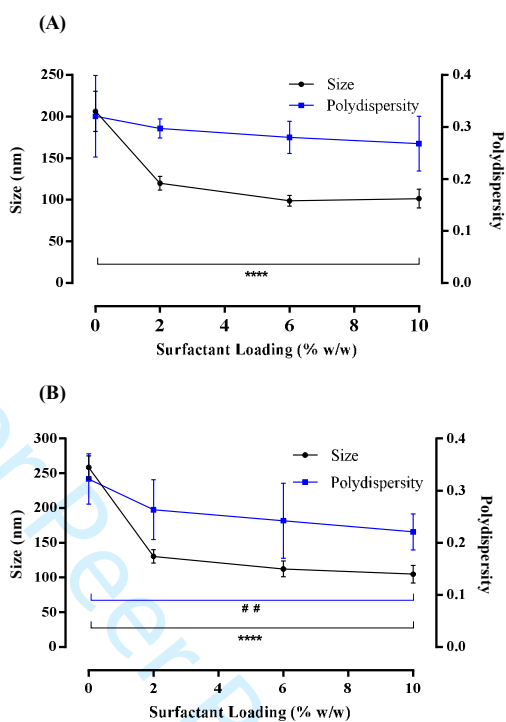


Fig. 1 Liposome size distribution and polydispersity of 'empty' and EGCG loaded liposomes

Liposome size distribution and polydispersity, determined by DLS, comparing (A) 'empty' and (B) EGCG loaded formulations with Tween 20 (0-10 % w/w). Liposomes were prepared by the dry film hydration method and EGCG added during the lipid mixing stage. Data represents mean \pm SD. n=3 independent batches. **** indicates statistical comparison between the size of liposome formulations with a $P \leq 0.0001$. ## indicates statistical comparison between the polydispersity of liposome formulations with a $P \leq 0.01$.

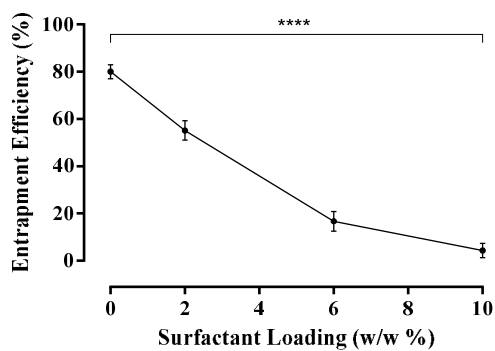


Fig. 2 Entrapment efficiency of EGCG in liposomes formulated with 0-10% w/w Tween 20

Entrapment efficiency (%) of EGCG in liposomes formulated with varying amounts of Tween 20 (0-10% w/w). Data represents mean \pm SD, n=3 independent batches. **** indicates statistical comparison between the entrapment efficiency of liposome formulations with a $P \leq 0.0001$.

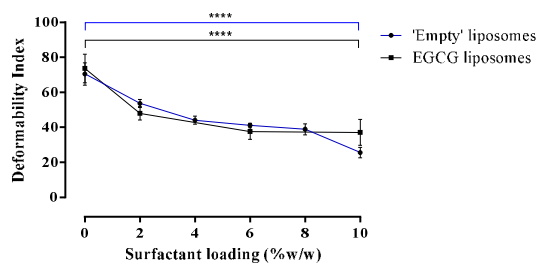


Fig. 3 Deformability index for 'empty' and EGCG loaded liposomes

Deformability index following extrusion through 50 nm membranes for 'empty' and EGCG loaded liposomes with increasing surfactant loading up to a maximum of 10% w/w. Liposomes were prepared adapting the dry film method adding the surfactant and adding EGCG during the lipid mixing stage. The preparation was vortexed and then extruded through the membranes. Data represents mean \pm SD. $n=3$ independent batches. **** indicates statistical comparison between the DI of liposome formulations with a $P \leq 0.0001$.

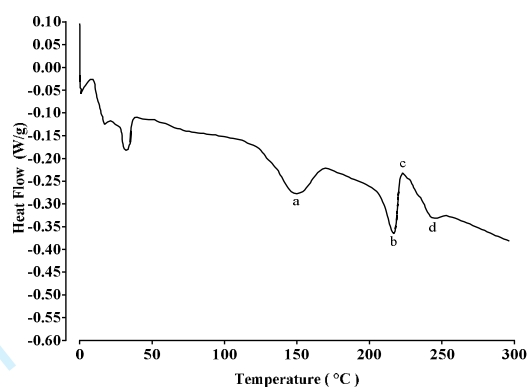


Fig. 4 Differential scanning calorimetry scan of EGCG

All experimental runs commenced at an initial temperature of 0 °C with a scan rate of 10 °C/min to 300 °C. Peak a and b are related to the epimer of EGCG, GCG. Peak c represents the glass transition temperature (T_g) of EGCG was at 220 °C and the melting point (T_m) of EGCG was at 245 °C.

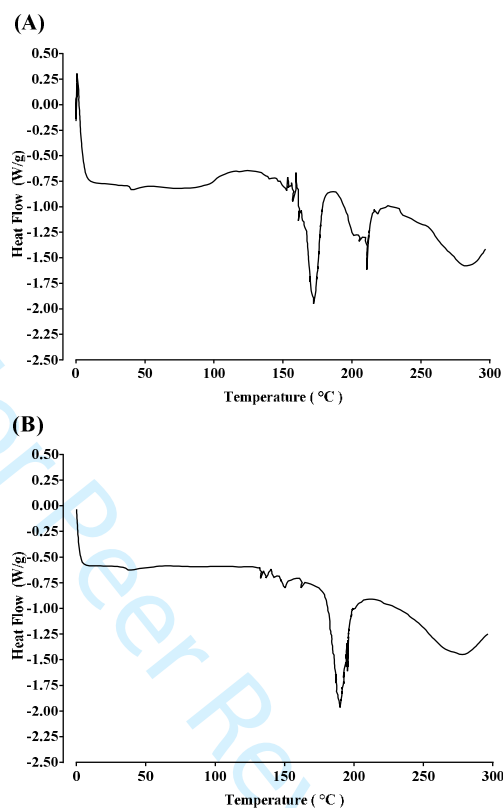


Fig. 5 Differential scanning calorimetry analysis scans of PC, cholesterol and Tween 20 and EGCG blends

DSC analysis scans of (A) PC, cholesterol and Tween 20 blend and (B) PC, cholesterol, Tween 20 and EGCG blend. The T_m of the lipid mixture is 172 °C, and upon addition of EGCG, the T_m was 191 °C. All experimental runs started at an initial temperature of 0 °C, purged under nitrogen gas, with a scan rate of 10 °C/min to 300 °C.

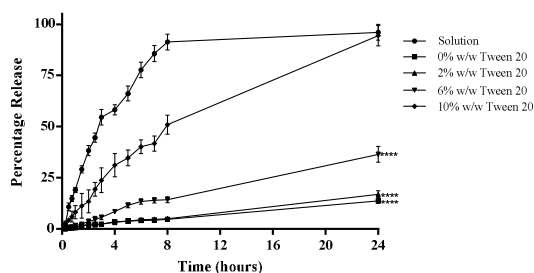


Fig. 6 *In-vitro* percentage EGCG cumulative release profiles from solution and liposomal formulations

EGCG release profiles from solution and liposomes formulated with 0, 2, 6 or 10 % w/w Tween 20 over 24 hours. Liposomes were prepared adapting the dry film method adding the surfactant and EGCG during the lipid mixing stage. A diffusion cell dialysis system was used to evaluate *in-vitro* drug release. Data represents mean \pm SD. n=3 independent batches. **** indicates statistical comparison between the EGCG release of liposome formulations with a $P \leq 0.0001$.

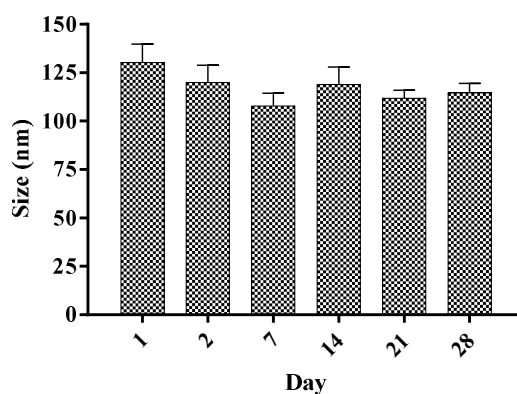


Fig. 7 Stability of EGCG loaded liposomes as determined by size

Size of EGCG loaded liposomes formulated with 0-10% w/w Tween 20, using DLS, formulated with up to 10% w/w Tween 20 measured on various days (1, 7, 14, 21 and 28). Data represents mean \pm SD. n=6 independent batches.

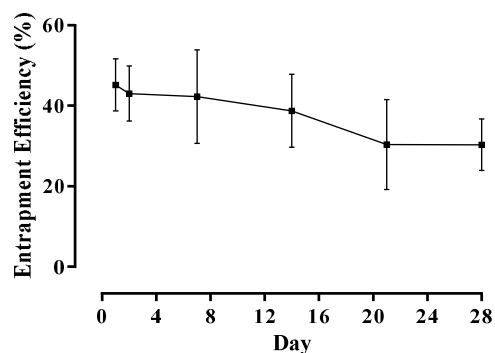


Fig. 8 Liposome encapsulation efficiency for EGCG

Liposome encapsulation efficiency for EGCG in liposomes formulated with 2 % w/w Tween 20 liposomes over 28 days. Liposomes were prepared adapting the dry film method adding the surfactant and drug during the lipid mixing stage. The preparation was then washed via centrifugation. The quantity of EGCG in supernatant over 28 days was then analysed by HPLC coupled with UV detection to assess liposome stability. Data represents mean \pm SD. n=6 independent batches.

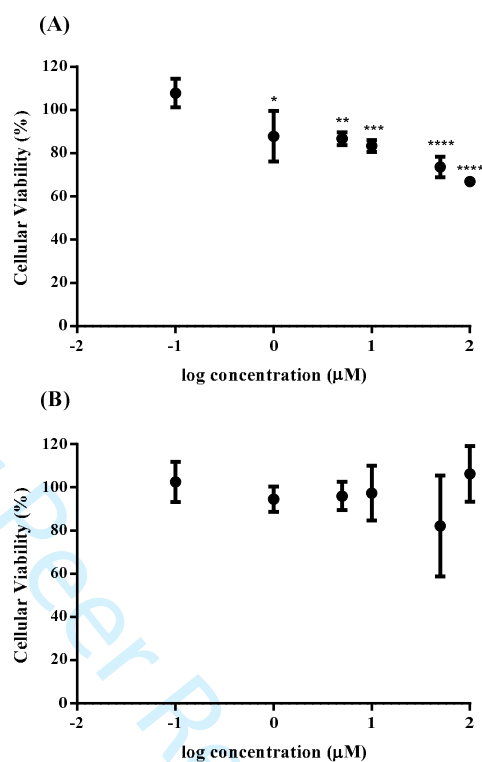


Fig. 9 Cellular toxicity of EGCG

HDFa (A) and HaCat (B) cells were grown on a 96-well plate at a density of 50×10^3 cells per well and exposed to various concentrations of EGCG (0.01-100 µM) for 24 hours. Thereafter 25 µL of a 12.5:1 parts mixture of XTT to menadione was added each well. Plates were incubated for 3 hours at 37°C and the absorbance read at 450 nm. Data is reported as mean \pm SD with 6 replicates per compound in at 3 independent experiments. ****, ***, **, * indicates statistical comparison between the entrapment efficiency of liposome formulations with a $P \leq 0.0001$, 0.001, 0.01 and 0.05 respectively.

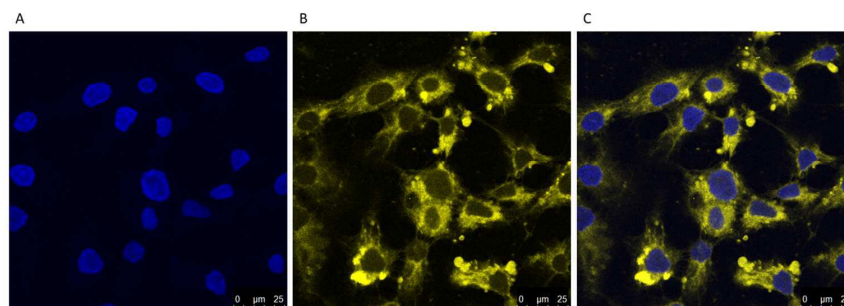


Fig. 10 Localisation of DiIc labelled liposomes loaded with EGCG and 2% w/w Tween 20 in HaCat cells

Cells were grown on the coverslips for 2 days. Cell nuclei were visualised using (A) DAPI (Blue). Liposomes were formulated with DiIc for visualisation (B) (yellow). Liposome localisation within the cell is shown in the merged image (C).

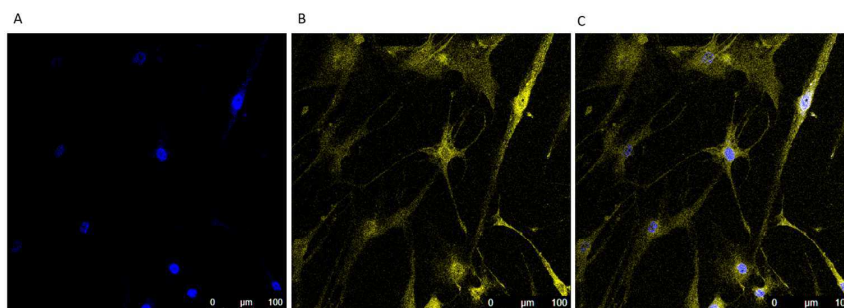


Fig. 11 Localisation of DiIc labelled liposomes loaded with EGCG and 2% w/w Tween 20 in HDFa cells

Cells were grown on the coverslips for 2 days. Cell nuclei were visualised using (A) DAPI (Blue). Liposomes were formulated with DiIc for visualisation (B) (yellow). Liposome localisation within the cell is shown in the merged image (C).